3

Stratosphere–Troposphere Coupling in the Southern Hemisphere

MARTIN JUCKER, PAULO CEPPI, DANIELA I. V. DOMEISEN, CHAIM I. GARFINKEL, EDWIN P. GERBER, EUN-PA LIM, AND ANDREW G. MARSHALL

3.1 Introduction

The lowermost 50 km of the atmosphere are traditionally divided into the troposphere (up to 12–16 km) and the stratosphere above that. In the troposphere, the temperature typically decreases with height due to an exponential decrease of pressure with height causing cooling via expansion following the first law of thermodynamics. Eighty percent of the total mass of the atmosphere is within the troposphere, and this is also where what we call the 'weather' occurs (see Chapter 1). In the stratosphere, the ozone layer absorbs most of the incoming ultraviolet radiation, which serves as a heat source for the stratosphere. As a consequence, temperature typically increases with height, causing the stratosphere to behave very differently from the underlying troposphere (Chapter 2). That chapter also touches on some of the influences the stratosphere can have in shaping surface weather and climate via connections between what is happening relatively high up in the atmosphere and at the surface. The present chapter will have its focus on these connections and interactions, which we will collectively call 'stratosphere–troposphere coupling'. While that coupling goes both ways, we will devote the majority of the chapter to the downward influence of the stratosphere on the troposphere.

Before describing the downward influence of the stratosphere, we introduce the main concepts and physical processes which govern stratosphere–troposphere coupling in Section 3.2 and then examine more specific phenomena related to downward stratospheric influence in the extratropics in Section 3.3 and the tropics in Section 3.4. More explicitly, we discuss the stratosphere's influence on tropospheric timescales and circulation (Section 3.3.1), before exploring the mechanisms behind the downward influence (Section 3.3.2) and surface impacts of stratospheric variability (Section 3.3.3). Section 3.4 concentrates on the tropospheric effects of and interactions with the tropical stratosphere, while Section 3.5 brings everything together and discusses how we can make use of stratosphere–troposphere coupling to improve on subseasonal to seasonal forecasting in the Southern Hemisphere (SH). We finish the chapter by describing some of the remaining challenges in Section 3.6.

3.2 Theoretical Background

3.2.1 Eliassen–Palm Flux

Interaction or coupling between the stratosphere and the troposphere takes place either via radiation, mass exchange, or the angular momentum carried by atmospheric waves propagating between the two layers. The latter is generally considered a dynamical coupling and will be the focus of this chapter.

In general, we define a perturbation as the difference between a given actual state of the atmosphere and a pre-defined background or base state. Probably the simplest way to define the base state is the zonal average, and the perturbed state is then defined by the deviations along that same zonal direction. Then, one can decompose the resulting perturbation into a spectrum of waves. Traditionally, that decomposition is done along the zonal direction using Fourier decomposition given the spherical symmetries and the common use of longitude-latitude-height coordinates. Therefore, the term 'wavenumber' is often implicitly used for the zonal wavenumber. To give a specific example, the actual state could be the geopotential height field at a given output time step from a climate model. The base state could then be the zonal mean geopotential height field at the same climate model time step, and the perturbation is the actual state minus the zonal mean. Another example of decomposing the same actual state would be to define the base state as the monthly average of the actual geopotential height field for, say, September 1981, or the September mean climatological geopotential height structure, say, from 1980 to 2009. Then, the perturbation can be the daily geopotential height minus the monthly base state for each day. In this case, the perturbation will have a zonally symmetric component, which will manifest itself through a non-zero amplitude of wavenumber 0, plus perturbations at each wavenumber as before with a zonally symmetric base state.

If one is interested in tropospheric dynamics, it is often sufficient to consider the horizontal propagation of waves. This has been very successfully applied to explain a wide range of tropospheric phenomena, such as tropical teleconnections (Hoskins and Karoly, 1981; Hoskins and Ambrizzi, 1993; Liu and Alexander, 2007). In our case, however, we are interested in the vertical coupling of two layers within the atmosphere, and therefore focus not on the longitude–latitude plane but the latitude–height plane (i.e., the zonally averaged atmosphere).

The derivation of vertical transfer of angular momentum via wave propagation in the atmosphere is generally attributed to Eliassen and Palm (1960). They considered the special case of stationary orographic gravity waves, but the physical concept is not limited to this exact application, and has later been generalised and linked to zonal mean acceleration (Andrews and McIntyre, 1976, 1978; Edmon et al., 1980), as well as the three-dimensional (Plumb, 1985; Takaya and Nakamura, 1997, 2001) and finite amplitude wave activity flux (Nakamura and Zhu, 2010; Lubis et al., 2018). Since its introduction, Eliassen–Palm (EP) flux has become a standard method of diagnosing vertical and meridional wave propagation as well as momentum transport.

The components of the EP flux vectors show the direction and strength of wave activity flux at a given position in latitude–vertical space. The meridional and vertical components are

$$\mathbf{F^p} \equiv (F_\phi, F_p) = \quad a\cos\phi(f_\phi, f_p), \tag{3.1}$$

$$\mathbf{F^z} \equiv (F_\phi, F_z) = \rho_0 a\cos\phi(f_\phi, f_z), \tag{3.2}$$

with

$$f_\phi = -\overline{u'v'} + \overline{u}_{z,p}\frac{\overline{v'\theta'}}{\overline{\theta}_{z,p}}, \tag{3.3}$$

$$f_{z,p} = \left(f - \frac{1}{a\cos\phi}\frac{\partial(\overline{u}\cos\phi)}{\partial\phi}\right)\frac{\overline{v'\theta'}}{\overline{\theta}_{z,p}} - \overline{u'\omega'}. \tag{3.4}$$

Bars denote zonal means and prime deviations from the zonal mean. ϕ is latitude, u, v are zonal and meridional wind, and θ is potential temperature. Subscripts z, p stand for vertical derivatives in either height (z) or pressure (p) coordinates. $f = 2\Omega\sin\phi$ is the Coriolis parameter and a Earth's radius. For pressure coordinates, ω denotes the pressure velocity (in Pa/s), and for height coordinates, it stands for the vertical velocity (in m s^{-1}, usually denoted w). Finally, $\rho_0 = \rho_s \exp(-z/H)$ is the density, and H the scale height.

In Equations (3.3) and (3.4), all but the first terms on the right-hand side are often neglected following quasi-geostrophic scaling, meaning that horizontal wave activity is directly related to meridional momentum flux $\overline{u'v'}$, whereas the vertical component is proportional to meridional heat flux $\overline{v'\theta'}$. While insolation at the top of the atmosphere is symmetric between the Northern and Southern Hemispheres, the circulation is rather different (Figure 3.1, also see Chapter 2): The SH winter stratospheric polar vortex is much stronger than its Northern Hemisphere (NH) counterpart (also see Chapter 2). This is because there is much stronger land-sea contrast in the NH, and there are more substantial mountain ranges, in particular the Tibetan Plateau, and thus much stronger, large-scale stationary waves (Hoskins and Karoly, 1981; Held et al., 2002; Garfinkel et al., 2020; White et al., 2021). As a result, the SH winter stratosphere is closer to radiative equilibrium, while the NH winter stratosphere is consistently warmer due to strong dynamical heating. This heating comes from large-scale atmospheric waves travelling from the troposphere into the stratosphere, where they break and deposit their angular momentum. As a result, the NH polar vortex is weaker, warmer, and more variable. Figure 3.1 shows climatological EP fluxes (vectors) and their divergence (shading) together with the resulting climatological zonal mean zonal wind (contours) for boreal and austral winter. Confirming the earlier discussion, EP fluxes and their divergence are weaker in the SH, while zonal winds are stronger compared to the NH.

In mathematical terms, this upward (i.e., troposphere to stratosphere) coupling is best described in the Transformed Eulerian Mean (TEM) formulation, which is particularly useful when discussing the effect of waves on atmospheric circulation (Andrews and McIntyre, 1976, 1978). It shows a direct link between zonal acceleration and the divergence of EP flux following

$$\frac{\partial\overline{u}}{\partial t} - f_0\overline{v}^* = \nabla\cdot\mathbf{F}, \tag{3.5}$$

where $\mathbf{F} \equiv (F_\phi, F_{z,p})$, and $\overline{v}^* = \overline{v} - (\overline{v'\theta'}/\overline{\theta}_{z,p})_{z,p}$ is the residual meridional wind. Equation (3.5) is the TEM equivalent to the traditional zonal momentum equation, and it links wave

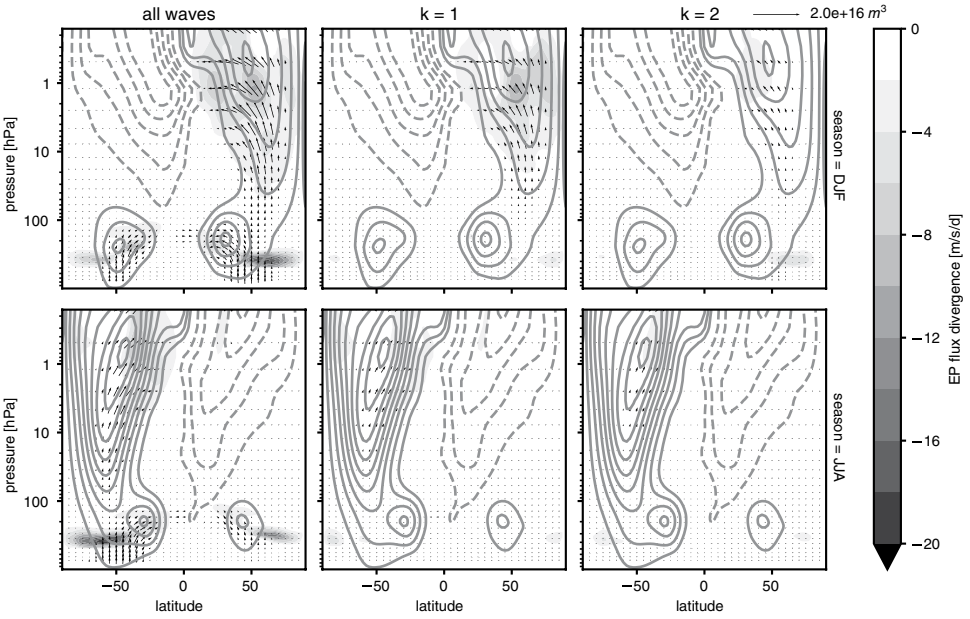

Figure 3.1 Climatological zonal mean zonal wind (contours), EP fluxes (vectors), and EP flux divergence (shading, negative only) for (top) boreal and (bottom) austral winters and for (left) all wave numbers, (middle) wave number 1, and (right) wave number 2. Zonal wind contours are shown from 100 to −100 m s^{-1} in 10 m s^{-1} intervals (dashed for easterlies), and EP flux divergence is shown in m s^{-1} day^{-1}. EP flux arrows are scaled following Jucker (2021) and an example scale is shown in the top right corner. These plots correspond to 1991–2020 seasonal climatologies from ERA5 reanalysis.

forcing (EP flux divergence) to zonal acceleration ($\overline{u}_t$) and meridional overturning circulation ($\overline{v}^*$). Therefore, Equation (3.5) is often interpreted as a form of wave-mean flow interaction, as the right-hand side ($\nabla \cdot \mathbf{F}$) represents waves, while the left-hand side represents the mean flow ($\overline{u}, \overline{v}^*$). At high latitudes, where the overturning circulation is preferentially downward and thus $\overline{v}^* \to 0$, EP flux divergence directly translates into zonal mean zonal wind acceleration. This is why in Figure 3.1, the strong zonal mean zonal wind in the SH polar stratosphere is accompanied by weak EP flux convergence, while the much weaker NH polar stratospheric zonal mean zonal wind coincides with strong EP flux convergence.

Not all waves can travel from the troposphere into the stratosphere. To show this, one can derive a refractive index for the zonal-mean vertical propagation of atmospheric waves (Charney and Drazin, 1961; Karoly and Hoskins, 1982). For simplicity, we consider the case of quasi-geostrophic flow with constant zonal mean zonal wind $\overline{u}$ and Brunt–Väisälä frequency N^2, assume plane waves, and make use of the Wentzel–Kramers–Brillouin (WKB) approximation (see, for instance, Vallis (2017)). Then, the potential vorticity equation can be solved for the vertical wave number m to obtain

$$m^2 = \frac{N^2}{f_0^2}\left(\frac{\beta}{\overline{u}-c} - K^2 - \frac{f_0^2}{4N^2H^2}\right), \tag{3.6}$$

where c is the phase velocity, $K^2 = k^2 + l^2$ the total horizontal wave number, and $\beta = f_y$. The condition for vertical propagation of waves is that the vertical wave number squared remains positive, that is, $m^2 > 0$, which yields

$$0 < \overline{u} - c < \frac{\beta}{K^2 + f_0^2 / 4N^2H^2} \equiv u_c, \tag{3.7}$$

known as the Charney–Drazin criterion (Charney and Drazin, 1961). It implies that stationary waves ($c = 0$) can only propagate upward if the prevailing winds are westerly ($\overline{u} > 0$) but weaker than the Rossby critical velocity u_c. Thus, for a given environmental wind structure, larger-scale waves (low K^2) will be able to propagate into the stratosphere, while smaller waves (large K^2) will be reflected back into the troposphere. Figure 3.1 illustrates how the total EP flux is dominated by small waves in the troposphere (many arrows in total tropospheric EP flux but no arrows in the troposphere for $k = 1$ and $k = 2$), while only the largest scales reach the stratosphere (total EP flux is dominated by $k = 1$ followed by some $k = 2$). This is the reason why differences in surface forcing between hemispheres are so important for the stratosphere: in the NH, the large-scale features of orographic forcing and land-sea contrast generate stationary waves with low wave numbers (so-called planetary waves due to their large horizontal scales), which find it easier to travel into the stratosphere than the relatively small-scale waves related to stochastic tropospheric turbulence (such as weather systems). In the SH, these large-scale stationary waves are weaker, resulting in a stronger winter polar vortex, as there is less wave propagation (Figure 3.1). However, this relation is circular, and it is often difficult to distinguish causation from co-occurrence: While fewer waves result in stronger background wind as just described, a stronger background wind also results in fewer waves because $\overline{u} > u_c$ for even lower K^2.

The $u = u_c$ contour is often called the 'critical line' as it marks the line where initially upward propagating waves cannot propagate anymore and break (as $\overline{u} - c \to 0$ the vertical wave number $m^2 \to \infty$). We note here that strictly speaking, the critical line only applies to linear theory, where the waves are of negligible amplitude, and in reality waves break before reaching $\overline{u} = c$. However, even for finite amplitudes, it is true that waves with smaller phase speed propagate closer to $\overline{u} = 0$ (Randel and Held, 1991). Also, Equation (3.7) explains why there are no arrows in the respective summer stratosphere in Figure 3.1, as the summer stratosphere features easterly winds, and no waves can travel from the troposphere into the stratosphere. Similarly, EP fluxes are concentrated within the waveguide formed by westerly winds ($\overline{u} > 0$), and start to diverge (point equatorward) where the zonal mean zonal wind reaches u_c. This is why the most important stratospheric feature for stratosphere–troposphere coupling is the stratospheric polar vortex (denoted SPV in this chapter), which will be at the centre of much of this chapter.

3.2.2 Downward Control

Up to now, we have discussed the upward influence of the troposphere onto the stratosphere. However, most of the remainder of this chapter is devoted to the downward influence of the stratosphere onto the troposphere. Following Holton et al. (1995), we can derive the

downward influence of divergent stratospheric EP flux by assuming steady-state ($\overline{u}_t = 0$) in the TEM formulation of Equation (3.5), and combining this with the conservation of mass via the continuity equation $\overline{v}^*_y + \rho_0^{-1}(\rho_0 \overline{\omega}^*)_z = 0$. Then, we require that there is no upward motion at the top of the atmosphere, for example, $\rho_0 \overline{\omega}^* \to 0$ as $z \to \infty$, to obtain

$$\rho_0 \overline{\omega}^* = -\frac{\partial}{\partial y}\left[\frac{1}{f_0}\int_z^\infty \rho_0 \nabla \cdot \mathbf{F} \mathrm{d}z'\right]. \tag{3.8}$$

This means that there is no upward residual motion above the wave forcing region, that is, above the last level where $\nabla \cdot \mathbf{F} \neq 0$, but any EP flux divergence (or convergence) forces a circulation throughout the column below the wave forcing region. In other words, any waves that leave the troposphere and eventually break in the stratosphere will drive a residual circulation in the troposphere. This phenomenon is called 'downward control', and is an important mechanism by which the stratosphere dynamically influences the troposphere. We note that most of the EP flux divergence in the stratosphere has its origin from tropospheric waves, meaning that in a way, the troposphere influences itself via the stratosphere. However, the stratosphere has an important role in regulating which waves propagate vertically, where they propagate towards, and where they eventually break.

These are simple diagnostics and theoretical concepts, and all of them suffer from a classic chicken-and-egg problem: Wave propagation is determined by the wind structure, but those same waves can alter the winds. Thus, as in many cases discussed in this chapter, EP fluxes and the TEM formulation can help diagnosing what is happening, but they can rarely distinguish between cause and effect or which was first, a change in winds or a change in waves. This is one reason why stratosphere-troposphere coupling is still a strong focus of contemporary research and will probably remain a challenging research topic for years to come, as discussed in Section 3.6.

After this general introduction into the theoretical frameworks often used to describe stratosphere–troposphere coupling, we will now discuss specific examples of stratosphere–troposphere coupling and show how the stratosphere influences tropospheric weather and climate on different time scales.

3.3 Stratosphere–Troposphere Coupling in the Extratropics

We start this section with a discussion of how the stratosphere influences the typical time scales of tropospheric variability. This is done by describing the behaviour of the entire troposphere as represented by the annular modes. We then discuss the mechanisms of the downward stratospheric influence and conclude with a review of the surface impacts of stratospheric perturbations.

3.3.1 Stratospheric Influence on the Annular Mode and Tropospheric Jetstream

The northern and southern annular modes (NAM/SAM) are the dominant patterns of variability in the extratropical atmosphere in each hemisphere, respectively (Hartmann and Lo, 1998; Thompson and Wallace, 2000). They characterise synoptic to subseasonal timescale

vacillations in the *position* of the jetstream in the troposphere and the *strength* of the polar vortices in the stratosphere. A meridional shift of the tropospheric jetstream is therefore often used as a synonym for a change in phase of the annular mode. Besides their intrinsic time scales discussed here, the annular modes can also be modulated by phenomena with much longer time scales, such as the El Niño Southern Oscillation (Chapter 11). The sign convention is that a positive annular mode indicates a stronger stratospheric polar vortex and poleward shift of the tropospheric jetstream, and vice versa for a negative annular mode. While the vertical structure of the NAM reveals coupling between the tropospheric jet and stratospheric vortex throughout the extended boreal winter, that is, from November to March, the SAM suggests that the coupling occurs much later in the season, that is, from October to January, peaking around October to November (e.g., Kushner, 2010; Lim et al., 2018; Son et al., 2013).

The annular modes are typically defined as the first Empirical Orthogonal Function (EOF) of zonal mean geopotential height poleward of 20° latitude, though nearly equivalent patterns can be found by computing EOFs of zonal mean zonal wind, or simply by computing mean geopotential height over the polar cap and regressing back on the full field, with suitable normalisation (Baldwin and Thompson, 2009; Gerber and Martineau, 2018). The associated Principal Component time series, or annular mode indices, characterise variability of the flow separately at each level. In the NH, the annular mode is referred to as the NAM, while in the SH, it is the SAM.

3.3.1.1 Internal Variability

Variability in the troposphere is quite barotropic, with all levels varying in concert. Baldwin and Dunkerton (2001) showed, however, that perturbations in the annular modes in the stratosphere tend to precede those in the troposphere by a few days. This coupling is pronounced during sudden stratospheric warming (SSW, see Chapter 2) events, when a collapse of the stratospheric polar vortex (a negative annular mode index above 100 hPa) precedes an equatorward shift in the jetstream (a negative annular mode index below 100 hPa). While major SSWs are very infrequent in the austral hemisphere (Jucker et al., 2021), similar linkages are observed with minor SSWs and the opposite strong and cold vortex events and around the time of the final warming, particularly if it is earlier in the season, and hence more dynamic in nature (Byrne et al., 2017; Byrne and Shepherd, 2018; Rao et al., 2020c).

Inter-hemispheric differences in the seasonality of stratospheric variability (peaking in mid-winter in the Northern Hemisphere versus late spring in the SH) cause an asymmetry in the annual cycle of stratosphere–troposphere coupling between the hemispheres. We quantify the coupling in Figure 3.2 via the annual cycle of the annular mode variance and persistence as a function of height (Baldwin et al., 2003; Gerber et al., 2010; Simpson et al., 2011a). The persistence of the annular mode is quantified by its *e*-folding time scale, that is, the typical period it takes anomalies in the stratospheric vortex or tropospheric jetstream to decay back towards climatology. In the NH, the time scale of the tropospheric annular mode peaks in mid-winter (Figure 3.2c), synchronous with higher variance in the stratospheric annular mode (Figure 3.2a), reflecting SSWs and strong

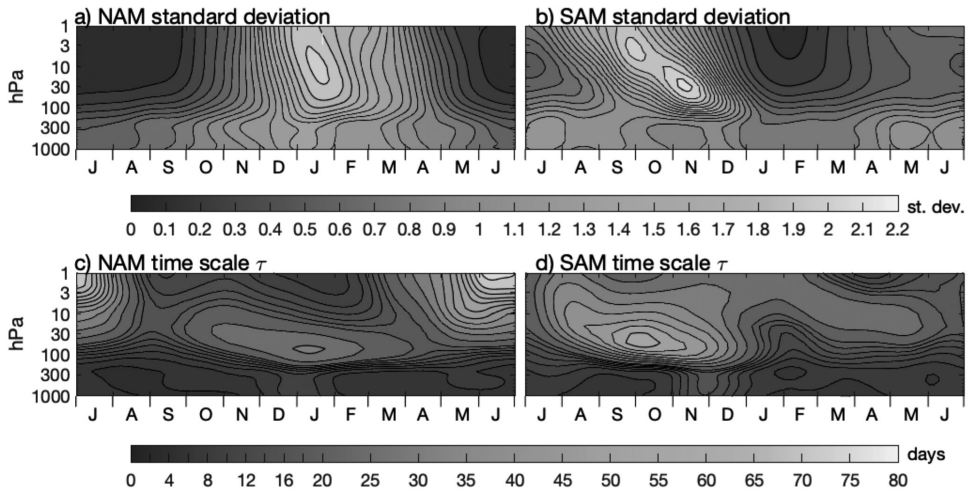

Figure 3.2 Coupling between the stratosphere and troposphere quantified by the annular modes. (a) and (b) show the annual cycle of variability in the Northern Annular Mode (NAM) and Southern Annular Mode (SAM), quantified by the standard deviation of the indices as a function of pressure and time of year. The indices are normalised to have unit variance at each level in the annual mean. (c) and (d) show the e-folding time scale of the annular mode as a function of time of year. See Baldwin et al. (2003) and Gerber et al. (2010) for further details. The results are based on the annular mode indices computed from JRA-55 reanalysis over the period 1958–2016, following Gerber and Martineau (2018).

and cold vortex events during this season (e.g., Horan and Reichler, 2017). The same pattern is observed in the SH, but delayed relative to the annual cycle: Enhanced time scales in the troposphere are observed in late spring (November–December; Figure 3.2d), again synchronously with peak variability of the annular mode in the lower stratosphere (Figure 3.2b; Jucker et al., 2021).

Gerber and Polvani (2009) established a causal link between enhanced variability of the stratospheric vortex and enhanced persistence of the annular mode in the troposphere. By systematically varying a simple topographic forcing in an idealised atmospheric model, they could control the variability of the stratospheric polar vortex. The annular modes reflected stronger coupling between the troposphere and stratosphere and more persistent variations of the tropospheric jetstream when topography was sufficiently large to perturb the stratospheric flow but not so large as to systematically destroy the vortex. The time scales of the annular mode in the stratosphere are always longer than in the troposphere, as the circulation is largely shielded from synoptic variability from below via the Charney–Drazin criterion (Equation 3.7). The enhanced persistence of the stratosphere can only impact the troposphere, however, where there is sufficient variability in the lower stratosphere. Breul et al. (2022) and Simpson et al. (2011a) demonstrated that the enhanced persistence of the SAM in November and December is associated in particular with variation in the timing of the final vortex breakdown. Specifically, Breul et al. (2022) showed that when one regresses out the tropospheric signal of final vortex breakdown from the annular mode index, the November–December peak in persistence vanishes.

3.3.1.2 Tropospheric Variability Forced by the Stratosphere

In addition to the coupling between the polar vortex and tropospheric jet reflected by internal variability (the annular modes), there is ample evidence from a hierarchy of models and observations that variations in the strength of the SH stratospheric vortex induce forced changes of the position of the tropospheric midlatitude jet. As a general rule, a stronger vortex leads to a poleward-shifted jet, consistent with a positive phase of the SAM. Arguably the clearest modelling evidence comes from idealised, 'dry dynamical core' simulations with imposed heating tendencies in the stratospheric polar cap, thus forcing changes in vortex strength, which result in annular mode-like tropospheric wind anomalies (Polvani, 2002). Qualitatively similar relationships were subsequently found in simulations of the atmospheric response to late twentieth-century polar stratospheric ozone depletion with both idealised and realistic global climate models (McLandress et al., 2011; Polvani et al., 2011; Garfinkel et al., 2023, also see Chapter 2).

Stratospheric ozone also plays an important role in forcing tropospheric changes independently of long-term ozone depletion and recovery. SPV anomalies induce polar cap ozone anomalies in the lower stratosphere. This is caused by the changes in polar temperatures and associated formation of polar stratospheric clouds on the one hand and meridional transport by the anomalous mean meridional overturning circulation on the other hand (Randel and Newman, 1998; Stolarski et al., 2005; Lim et al., 2018; Fogt and Marshall, 2020): Weakening of the springtime SPV is associated with enhanced ozone concentration in the polar cap region from spring to early summer, and strengthening of the spring polar vortex is associated with decreased polar ozone concentration. Ozone anomalies in turn can have an influence on static stability in the lower stratosphere, which modifies the vertical propagation of planetary waves and ultimately modifies the tropospheric circulation via downward control (Section 3.2; Jucker and Goyal, 2022). Importantly, ozone anomalies driven by the vortex anomalies can positively feed back into the vortex-driven polar cap temperature anomalies, and therefore modulate the meridional temperature gradient in the lower stratosphere and the troposphere. This again promotes a meridional shift of the tropospheric eddy-driven jet, that is, a change in the annular modes (Son et al., 2013; Hendon et al., 2020; Oh et al., 2022; Friedel et al., 2022). Hendon et al. (2020) and Oh et al. (2022) demonstrated in their modelling studies that ozone anomalies play a key role in modulating the Antarctic vortex breakdown dates and amplifying the responses of the SAM and associated surface climate anomalies to the stratospheric vortex anomalies.

Observational analyses also show a clear interannual relationship between stratospheric vortex breakdown date and tropospheric zonal-mean jet latitude during austral summer (Byrne et al., 2017; Ceppi and Shepherd, 2019). The breakdown date of the SH stratospheric vortex (as measured in the lower stratosphere at 50 hPa) strongly correlates with its strength in late spring (November–December), when interannual vortex variability is largest. Although interannual correlations alone cannot demonstrate causality, lagged regression analysis reveals a downward propagation of the stratospheric wind anomalies associated with interannual vortex strength variations, consistent with the tropospheric jet shift peaking a few weeks after the stratospheric vortex anomalies (Figure 3.3a–c; Byrne et al., 2017). The downward influence is further confirmed by causal network analysis,

where an increase in tropospheric SAM timescales could be explained with a statistical model in which downward influence was included but tropospheric autodependence was excluded (Saggioro and Shepherd, 2019).

Although the tropospheric jet response to stratospheric vortex strengthening is typically understood as a poleward shift, in the context of SH summer, this response is better described as a delayed equatorward transition over the course of the seasonal cycle. Every year, following the vortex breakdown in late spring, the tropospheric jet transitions to a more equatorward position in early summer, but this transition is delayed in years where the vortex breaks down later than average, and vice versa (Byrne et al., 2019). This interannual coupling between vortex breakdown and the regime transition of the tropospheric jet supports the idea that the former drives the latter, although it is possible that drivers other than the stratospheric vortex also contribute to the tropospheric jet transition.

Similarly, the jet response to polar stratospheric cooling associated with ozone depletion is best explained as a delayed equatorward transition in early austral summer, as opposed to a coherent poleward shift across the entire summer (Sun et al., 2014). CO_2 forcing also causes polar stratospheric cooling and hence a vortex strengthening, but the magnitude of this strengthening is highly uncertain in global climate models (cf. Figure 3.1b in Ceppi and Shepherd, 2019; Mindlin et al., 2021). Ceppi and Shepherd (2019) demonstrated how the stratospheric vortex response to CO_2 forcing contributes to the poleward jet shift in austral summer, both in terms of the mean response (accounting for almost half of the poleward shift) and its spread (explaining about 30% of the inter-model variance). As shown in Figure 3.3d–f, the tropospheric impact of the stratospheric vortex response simulated in a twenty-first-century global warming scenario (RCP8.5) is strikingly similar to that observed in response to an interannual change in the vortex (Figure 3.3a–c), supporting the idea that the same dynamical mechanisms are at play. A similar downward influence on the simulated tropospheric jet response to CO_2 forcing was found in NH winter (Simpson et al., 2018). Note that the causes of this model uncertainty in stratospheric vortex response remain unexplained and may be related to tropospheric circulation changes earlier in the season.

3.3.2 Mechanisms of the Downward Influence

For the initial downward propagation of anomalies within the stratosphere, wave-mean flow interactions on the critical line (see Section 3.2) can lead to gradual downward movement of the Antarctic wind and temperature anomalies from the lower mesosphere and the upper stratosphere into the lower stratosphere (Randel and Newman, 1998; Baldwin and Dunkerton, 2001; Dowdy, 2004; Thompson et al., 2005; Dowdy et al., 2007; Byrne and Shepherd, 2018; Lim et al., 2018, and references therein). For instance, weakening of the springtime SPV reduces zonal wind strength, and therefore sets a lower critical line for the upward propagation of planetary-scale waves. This causes subsequent waves to break at a lower level than the previous waves and to further weaken the SPV, which lowers the critical line further, and so on.

As discussed in the introduction to this chapter, the downward influence of the stratosphere on the troposphere is effected by a combination of synoptic and planetary scale

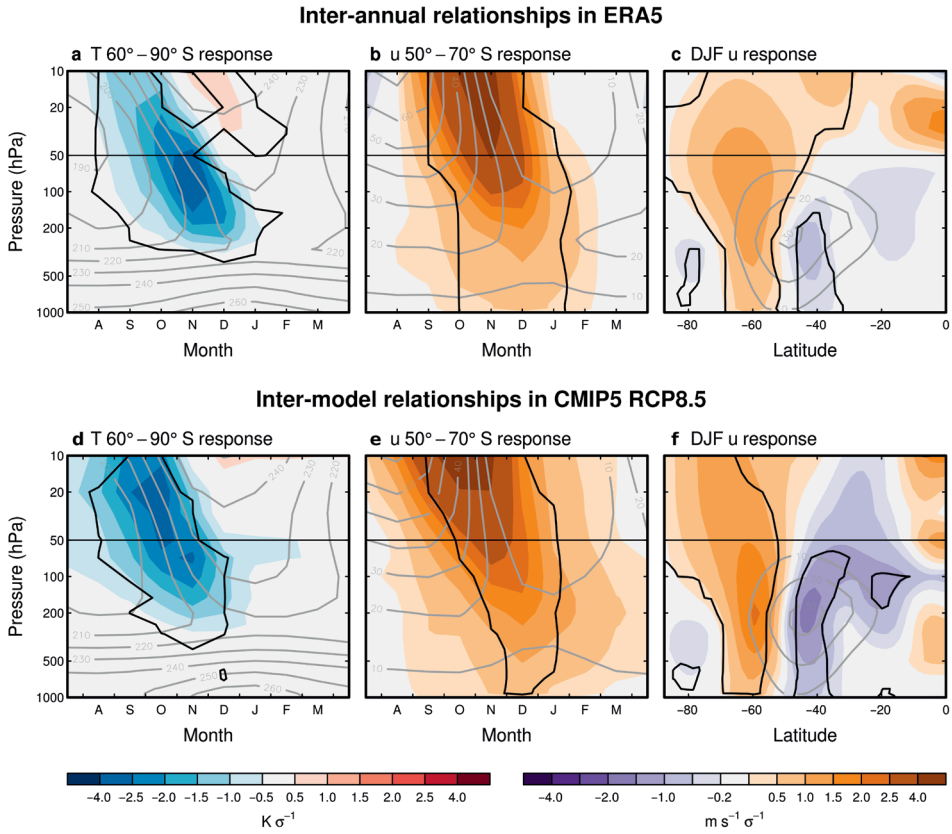

Figure 3.3 (a–b) Interannual regression coefficients of (a) polar cap temperature at 50 hPa and (b) 50°–70°S zonal-mean zonal wind at 50 hPa onto the vortex breakdown date (in calendar days), between July 1979 and June 2018. The vortex breakdown date is defined as the final time when the daily-mean, zonal-mean zonal wind at 50 hPa and 60°S drops below 15 m s^{-1}. (c) shows the December–February (DJF) zonal-mean zonal wind as a function of latitude and pressure, regressed onto the vortex breakdown date. (d–f) as in panels (a–c), but regressing temperature and zonal wind *responses* onto vortex breakdown date responses, across CMIP5 climate models in the RCP8.5 scenario. For each model, the responses are calculated as the difference between years 2080 and 2099 of RCP8.5 and the mean pre-industrial control climate. In all panels, the regression coefficients are standardised according to the standard deviation σ of the vortex breakdown date, calculated either across years (panels a–c) or across CMIP5 models (d–f). Adapted from Ceppi and Shepherd (2019). Reprinted with permission from John Wiley and Sons © 2019. The Authors.

eddies. Synoptic transient eddies underlie the annular modes and, in particular, both drive and subsequently maintain a jet shift whether or not the shift is forced (Hartmann and Lo, 1998; Lorenz and Hartmann, 2001; Gerber and Vallis, 2007). Synoptic waves may also be directly affected by the stratosphere (Yang et al., 2015). In addition to the synoptic eddies, planetary waves appear to contribute to the downward propagation of the signal from the stratosphere (Martineau and Son, 2015).

Planetary waves include both transient planetary waves and stationary planetary waves forced by zonal asymmetries in the lower boundary of Earth's surface. As described in Section 3.2, the climatological stationary waves in the SH winter are much weaker than those in the NH. However, from September to November, the SH polar vortex is weaker than in winter while tropospheric stationary waves are strong, and as a result stratospheric stationary waves are of comparable strength to those in the NH (Figure 3.1). The largest interannual variability of the SH stratospheric circulation is also observed in austral spring when the planetary waves are most active as compared to other seasons, and on rare occasions the westerly jet reverses in a sudden warming also in this season (Allen et al., 2006; Rao et al., 2020c; Shen et al., 2020; Lim et al., 2021; Jucker and Goyal, 2022).

Transient planetary waves have been shown to encourage the downward impact (Martineau and Son, 2015). For example, Smith and Scott (2016) find that the response to a stratospheric perturbation is weaker if interactions between planetary- and synoptic-scale waves are suppressed, while Domeisen et al. (2013) find that the jet shifts in the opposite direction if only planetary waves are present, ruling out the possibility that the jet shift occurs purely as a response to changes in the planetary- or synoptic-scale wave fields alone.

While the role of stationary waves has received less attention, recent work has demonstrated they also play a role and weaken the surface response (Hitchcock et al., 2013; Garfinkel et al., 2023). The net effect is that stationary waves weaken the circulation response to ozone depletion in both the stratosphere and troposphere and also delay the response until summer rather than spring when ozone depletion peaks. This effect arises because stationary waves negatively feed back on the imposed stratospheric perturbation and weaken it if stationary waves are forced by the bottom boundary. That is, as the vortex strengthens, it allows more upward wave activity into the stratosphere, and this reservoir of wave activity is larger if stationary waves are present. Even though SH stationary waves are weaker than their NH counterparts, they nonetheless are crucial for regulating the net response to ozone depletion.

3.3.3 Surface Impact of Dynamical Stratospheric Perturbations

As discussed in Section 3.3.1, the primary signature of tropospheric circulation anomalies resulting from the SH stratosphere–troposphere coupling is a meridional shift of the tropospheric eddy-driven jet: An unusually weak and warm springtime SPV extends downward in the Antarctic circumpolar region, leading to equatorward shifts of the tropospheric eddy-driven jet and associated midlatitude storm track, thereby decreasing surface pressure in the midlatitudes but increasing it in the Antarctic region, which characterises the negative phase of the SAM (Figures 3.4a,b). An unusually strong and cold springtime SPV leads to the positive phase of the SAM with the oppositely signed changes. Although the downward coupling of the SH SPV anomalies can be zonally asymmetric (e.g., Black and McDaniel, 2007; Shaw et al., 2010), the SAM is a main pathway for the springtime SPV variability to impact the SH surface climate on a seasonal time-scale, providing

long-lead predictability of surface climate anomalies up to a season in advance (Lim et al., 2018, 2021).

The relationships of the SH late spring tropospheric circulation and surface climate anomalies with the spring SPV weakening (which occurs with polar warming) are demonstrated by regressing October to December-mean anomalies of zonal winds and vertical velocity at 500 hPa, mean sea level pressure, precipitation, and 2-m temperatures onto the inversely signed September to November-mean zonal-mean zonal wind anomalies at 60°S and 10 hPa (e.g., Seviour et al., 2014) (Figure 3.4). The nearly zonally symmetric meridional dipoles of tropospheric zonal wind and mean sea level pressure anomalies in the regression pattern characterise the negative phase of the SAM with enhanced zonal winds and decreased pressures in the midlatitudes equatorward of 50°–55°S and the opposite changes in the latitudes poleward of that latitude band. This SPV-SAM connection was demonstrated to be robust when compositing earlier-than-normal SPV breakdown events (SSWs) from a multi-millennial coupled-model simulation (Jucker and Reichler, 2023). Precipitation anomalies associated with the SPV also bear the resemblance to the zonal wind and pressure anomalies in the extratropics, being consistent with an equatorward shift of the storm track during the negative phase of the SAM. On the other hand, 2-m temperature anomalies associated with the SPV display zonally asymmetric anomalies, especially with a strong zonal dipole of temperature anomalies east and west of the Amundsen Sea, which reflects the zonally asymmetric component of the SAM (Campitelli et al., 2022). In accordance with the zonal dipole of the temperature anomalies in the west Antarctic region, sea-ice tends to decrease over the eastern Ross-western Amundsen Seas but to increase over the Weddell Sea in the austral early summer season of November to January when the spring SPV is weaker and warmer than normal (Lim et al., 2018).

Also, bands of significantly higher temperature and reduced rainfall across Australia, subtropical South America, and parts of South Africa are found in Figures 3.4c,e. This is associated with an equatorward shift of the downward branch of the SH Hadley cell and resultant increased downward motion in the SH subtropical latitudes during the negative phase of the SAM (Kang et al., 2011; Ceppi and Hartmann, 2013; Hendon et al., 2014), which can be driven by weaker spring SPVs (Figure 3.4d; e.g., Lim et al., 2019a; Lim et al., 2021). It is noteworthy that the subtropical anomalies are particularly pronounced over eastern Australia, which is not only affected by the Hadley cell edge but also by the local circulation over the Tasman Sea that modulates the moisture inflow to eastern Australia associated with the SAM (Hendon et al., 2007).

Bandoro et al. (2014) and Lim et al. (2019a) showed that when the spring SPV is anomalously weak and the SAM is negative, the chances of extreme high temperatures and extreme low rainfall are significantly increased in the following late spring to summer seasons over eastern Australia. Consequently, the chance of forest fire-conducive weather conditions also tends to significantly increase when the SPV is significantly weaker and warmer than normal (Lim et al., 2019a). For instance, severe forest fire incidents that occurred over far eastern Australia during the austral late spring of 2019 were attributable to the hot and dry conditions promoted by the near-major SSW of spring 2019, according to a statistical model (Lim et al., 2021).

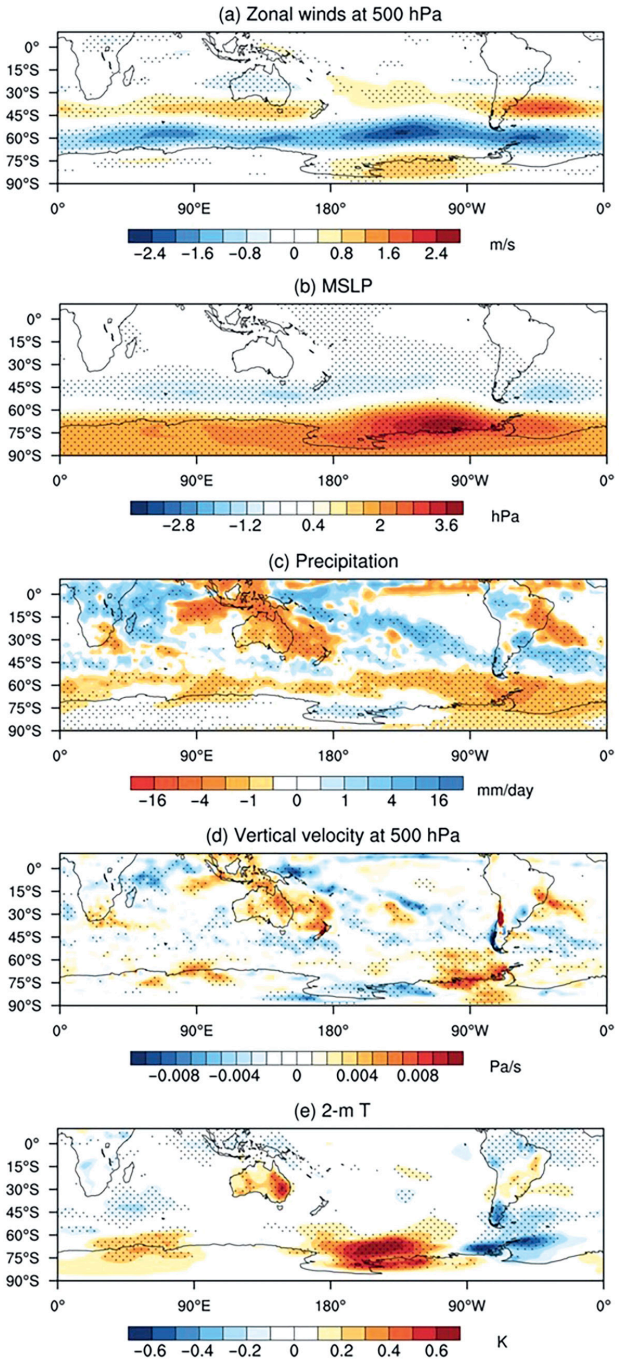

Figure 3.4 Regression of October–December mean anomalies of (a) zonal winds at 500 hPa, (b) sea level pressure, (c) precipitation, (d) vertical velocity at 500 hPa, and (e) 2-m temperatures onto the inversely signed spring (September–November) SPV (zonal wind anomalies at 60°S and 10 hPa) over the period 1979–2021. The SPV index sign was reversed to show the circulation and surface climate anomalies associated with the vortex weakening. The red colour shading indicates westerlies, higher pressures, downward motion, lower precipitation, and higher temperature anomalies, and the blue colour shading indicates the opposite. Stippling indicates statistically significant regression at the 10% level as assessed by a two-tailed Student t-test with 43 samples.

3.4 The Tropical Stratosphere: Interactions between the Quasi-Biennial Oscillation and the Troposphere

After discussing the downward influence of the stratosphere via the strength of the stratospheric polar vortex, we now turn our attention to tropospheric effects of, and interactions with, the tropical stratosphere. In this section we explore the strong connection between the stratospheric Quasi-Biennial Oscillation (QBO; Ebdon, 1960; Baldwin et al., 2001) and the tropospheric Madden–Julian Oscillation (MJO; Madden and Julian, 1971) before discussing remote influences of the QBO on the SH extratropics. The QBO is a prominent oscillation that describes a descending reversal of the zonal-mean zonal wind in the tropical stratosphere and represents the main mode of variability in the tropical stratosphere (see Chapter 2).

3.4.1 Interactions between the Quasi-Biennial Oscillation and the Madden–Julian Oscillation

Alternating between its easterly (QBOE) and westerly (QBOW) phases over a period of around 28 months (e.g., Baldwin et al., 2001), the QBO at 70 hPa (e.g., Kuma, 1990) and 50 hPa (e.g., Yoo and Son, 2016; Martin et al., 2021; Haynes et al., 2021) is shown to modulate the year-to-year variability of the boreal winter MJO. This strong and significant relationship appears to be unique to the MJO, with no other mode of tropical convective variability showing a statistically significant connection to the QBO (Christiansen et al., 2016; Son et al., 2017; Abhik et al., 2019; Sakaeda et al., 2020; Haynes et al., 2021). We synthesise observational understanding of the QBO-MJO relationship, possible mechanisms behind the connection, and its modulation of extratropical teleconnections forced by the MJO. We then discuss simulations of the QBO-MJO relationship in global climate models and some of the gaps in our understanding that should be considered in future research. The QBO-MJO relationship can also be used in subseasonal-to-seasonal predictions, which will be discussed in Section 3.5.

Observations indicate that the MJO is about 40% stronger and persists for about 10 days longer when QBO winds at 50 hPa are easterly, compared with the westerly QBO phase (e.g., Martin et al., 2021). These changes translate to a 20–40% increase in the strength of MJO rainfall anomalies, for both the active and suppressed convection phases of the MJO, during QBOE (Yoo and Son, 2016). Besides a stronger and more active MJO (Figure 3.5), QBOE years also tend to show slower eastward propagation that reaches further into the western Pacific than during QBOW years (e.g., Yoo and Son, 2016; Son et al., 2017; Nishimoto and Yoden, 2017; Zhang and Zhang, 2018; Wang et al., 2019). Overall, the QBO at 50 hPa accounts for almost half of the MJO's interannual variance from December to March, while outside the boreal winter season, the QBO-MJO relationship is substantially weaker (Wang et al., 2019).

Further, while the QBO-MJO connection appears to be a stable feature of the present climate, there exists no evidence of a relationship prior to the 1980s. Although observational data are sparse further back in time, extended analyses for earlier periods suggest a role for anthropogenic climate change in sensitising MJO convection to variability in the QBO at

50 hPa since the early 1980s (Klotzbach et al., 2019; Sakaeda et al., 2020). Specifically, cooling of the tropical lower stratosphere and warming of the upper troposphere, and/or a change in the vertical structure of the MJO, may have provoked the QBO-MJO connection to emerge at this time.

3.4.1.1 Proposed Mechanisms

There exists an expanding body of literature that seeks to understand the key observational features of the QBO-MJO relationship, namely its boreal winter seasonality, its emergence in the 1980s, and the significance of the connection to the MJO but to no other mode of tropical convective variability. However, despite the robustness of the QBO-MJO link in observations, there is no consensus to date on a single mechanism that can explain these features. Several possible mechanisms have been suggested, the most frequently explored being the stratification of temperature in the upper troposphere-lower stratosphere region by the QBO at 50 hPa, and its subsequent impact on MJO convection (e.g., Son et al., 2017; Hendon and Abhik, 2018). In this scenario, adiabatic cooling during EQBO drives cold temperature anomalies that decrease the static stability near the tropopause, thereby promoting stronger MJO convective activity, while adiabatic warming during WQBO has the opposite effect.

Another possible contributor to the QBO-MJO connection includes radiative feedbacks from high-altitude cirrus clouds, which radiatively cool the lower stratosphere and warm the troposphere (e.g., Hartmann et al., 2001; Yang et al., 2010; Hong et al., 2016). Since these clouds form more readily over the Indo-Pacific warm pool during QBOE when the tropopause is colder than during QBOW, they may further destabilise the upper troposphere to promote MJO deep convection (e.g., Son et al., 2017; Sun et al., 2019). Other proposed mechanisms suggest a role for QBO wind anomalies at lower-stratospheric levels in altering the behaviour of atmospheric wave breaking, propagation, reflection, and/or attenuation and their subsequent influence on tropical convection (e.g., Lane, 2021); however, further work is required to fully understand their potential impact on the MJO. All these hypotheses are built on the assumption that it is the QBO that influences the MJO, and not the MJO modulating the QBO. Indeed, lead-lag analyses show that QBO signals at 50 hPa affect changes in the MJO about two months later (Son et al., 2017), even though there are currently no theories of this relationship.

3.4.1.2 Global Influences

In addition to its local influences on MJO behaviour, the QBO at 50 hPa is also shown to induce changes to the MJO's extratropical teleconnection patterns. In the NH, MJO-induced atmospheric Rossby wave trains over the North Pacific (e.g., Matthews et al., 2004) become better organised and more pronounced during QBOE than during QBOW (e.g., Son et al., 2017; Wang et al., 2018; Toms et al., 2020). This is likely to influence the MJO's modulation of the North Pacific storm track, which becomes more longitudinally elongated and intense during QBOE (Wang et al., 2018). The MJO's influence on circulation and rainfall in East Asia also strengthens and becomes more organised during QBOE, leading to QBOE-QBOW differences in precipitation of around 40–70% (Kim et al., 2020b). In the SH, the South Atlantic Convergence Zone intensity and precipitation over southeastern

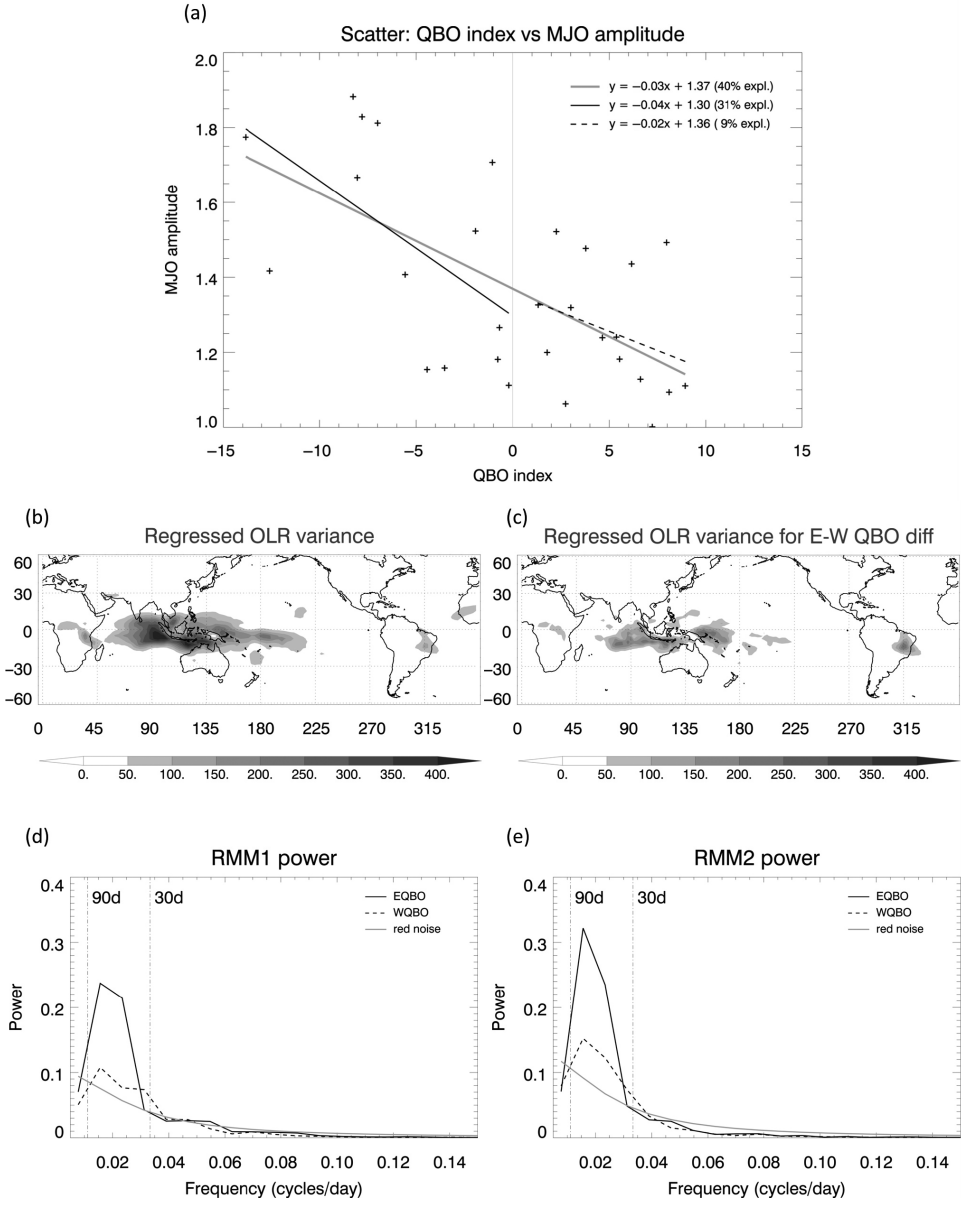

Figure 3.5 (a) Scatter plot for QBO index versus MJO amplitude using NCEP-NCAR Re-analysis data (Kalnay et al., 1996), 1981–2010, where each marker represents a DJF seasonal mean. Linear regression fits to the data are shown over the full dataset (solid grey line), for the easterly QBO phase (solid black line), and for the westerly QBO phase (dashed black line). Corresponding regression equations are also given, and the variance in MJO amplitude explained by the QBO is shown in parentheses. Spatial maps of variance for anomalous outgoing longwave radiation (OLR) regressed onto the Realtime Multivariate MJO index pair, RMM1 and RMM2 (Wheeler and Hendon, 2004), (b) using all daily data and (c) using subsets of the data to show the difference in variance for easterly minus westerly QBO phases for DJF, 1981–2010 (W^2 m^{-4}). Power spectra of (d) RMM1 and (e) RMM2 for the easterly QBO phase (solid black line) and for the westerly QBO phase (dashed black line). The solid grey lines represent red noise spectra, and periods of 30d and 90d are indicated. Reproduced from Marshall et al. (2017) with permission from Copyright © 2016, Springer-Verlag Berlin Heidelberg.

South America are known to be impacted by the MJO (Carvalho et al., 2004), and they are intensified during MJO phases 1 and 4 in particular for QBOE, whereas the extratropical wave response associated with the anomalous convection over the Maritime Continent is larger during MJO phase 4 for QBOW (Sena et al., 2022). These examples highlight the diversity of QBO impacts on MJO teleconnections and the challenges presented in elucidating the possible mechanisms at play (Martin et al., 2021). Disentangling QBO changes to the background state from QBO-induced changes to the MJO itself remains key to better understanding the QBO-MJO connection and its influences on global climate.

3.4.2 Influence of the Quasi-Biennial Oscillation on the Southern Hemisphere Extratropics

In addition to the impact of the QBO on the MJO, the QBO also impacts seasonal mean conditions through at least two pathways: (1) changes in the stratospheric polar vortex and (2) changes in seasonal mean tropical convection and an associated extratropical Rossby wave train.

3.4.2.1 QBO-SH Midlatitude Impacts via the Polar Vortex

The SH SPV is affected by the QBO. The Antarctic stratosphere is warmer from late winter to spring, and the final warming occurs earlier, when the QBO is in its easterly phase near 20 hPa, and vice versa for the westerly phase (Baldwin and Dunkerton, 1998; Gray et al., 2018; Yamashita et al., 2018 Naito, 2002; Hitchman and Huesmann, 2009; Anstey and Shepherd, 2014). Namely, seasonal westerly deceleration in the SH stratosphere in spring is faster during QBOE conditions than QBOW. While this modulation of the vortex is induced by anomalous propagation of Rossby waves (e.g., Rao et al., 2023), the causal mechanism(s) behind this connection are still unclear. Further, the QBO regime with the strongest impact on the SH vortex is different from that in the NH (20 hPa in the SH and 50 hPa in the NH), and even in the NH there is no consensus on which mechanism might be most important.

Regardless of the mechanism, a consequence of the effect of the QBO on the SPV is that the SAM is also influenced by the QBO, thus translating the tropical stratospheric QBO signal into one of surface climate (Naito, 2002; Roscoe and Haigh, 2007; Anstey and Shepherd, 2014; Anstey et al., 2022; Rao et al., 2023): QBOE conditions at 20 hPa are associated with a negative SAM, while QBOW conditions are associated with a positive SAM in late spring and summer. The surface impacts are similar to those described in Section 3.3.3 and are not repeated for brevity.

3.4.2.2 QBO-SH Midlatitude Impacts Via Seasonal Mean Tropical Convection

The QBO is known to alter tropical outgoing longwave radiation and precipitation on seasonal mean timescales (Giorgetta et al., 1999; Collimore et al., 2003; Liess and Geller, 2012; Rao et al., 2023). This convection pathway appears to be particularly pronounced if QBO regimes are defined using winds at 70 hPa, likely because of the proximity to the tropical tropopause layer (Gray et al., 2018; Peña-Ortiz et al., 2019). Nevertheless, some studies focus on other QBO regimes due to the inability of most models to simulate a QBO

to the lowermost stratosphere (Richter et al., 2020; Rao et al., 2020a, 2020b). The specific mechanism(s) involved in this downward impact on seasonal mean convection is likely to be similar to the mechanism(s) for its impact on the MJO discussed in Section 3.4.1.

The response to the QBO tends to be concentrated in the region with climatologically deepest convection. In austral winter, this region is over the South and East Asian monsoons extending towards the Philippines, and in austral summer, it is over the Maritime Continent and western Pacific (Giorgetta et al., 1999; Yamashita et al., 2018; Peña-Ortiz et al., 2019; Rao et al., 2020a). Defining the QBO at a higher level can lead to a qualitatively different convection response (Gray et al., 2018), possibly because there exist multiple mechanisms whereby the QBO can affect convection.

The localisation of the convection response can launch a Rossby wave train that propagates from the tropics to the extratropics (Peña-Ortiz et al., 2019; Yamazaki and Nakamura, 2021; Rao et al., 2023). In austral winter (June-August), the wave train associated with QBOE includes a ridge off the east coast of subtropical Africa, a deepened low in the midlatitude Indian Ocean sector, a ridge north of Australia, and a strong trough near the dateline off the coast of Antarctica (Yamazaki and Nakamura, 2021). The overall response to the QBO resembles zonal wave-3 in June through August. In spring (i.e., after the vortex route becomes active), on the other hand, the wave train is qualitatively different, likely due to its superposition on the SAM response associated with the polar vortex (Rao et al., 2023). The net effect is that the SAM response associated with QBOE (higher heights in subpolar latitudes and lower heights in midlatitudes) is less zonally symmetric compared to a typical SAM and is instead concentrated in the Indo-Pacific sector.

This wave train affects surface climate. The subpolar ridge in the Pacific sector during QBOE leads to warmer temperatures over East Antarctica (likely due to strengthened advection of maritime air) and colder temperatures near the Antarctic Peninsula and West Antarctica (Rao et al., 2023). The composite difference of sea ice concentrations between QBOE and QBOW in June through August shows positive anomalies over the Ross Sea and Weddell Sea (Yamazaki and Nakamura, 2021), a response that is also associated with atmospheric circulation anomalies induced by the enhanced convection in the tropical Indian Ocean.

3.5 Subseasonal-to-Seasonal Predictability in the SH Stratosphere–Troposphere Coupled System

The stratosphere has been recognised as an important precursor for both variability (this chapter) and extremes (Domeisen and Butler, 2020) in surface weather on timescales of weeks to months (in addition to longer timescales, mostly related to stratospheric ozone trends and extremes (Thompson et al., 2011; Calvo et al., 2015), which will not be the focus here). Since the stratosphere evolves more slowly as compared to the underlying troposphere (Gerber et al., 2010; Domeisen et al., 2020b, Section 3.3.1), the stratosphere is a promising source of predictability on so-called *subseasonal to seasonal (S2S)* timescales (Merryfield et al., 2020; Scaife et al., 2022), corresponding to the timescales of a few weeks to months. S2S prediction had been identified as a 'predictability desert' with respect to other timescales such as the

shorter weather and longer climate timescales, where prediction is more established. A surge in S2S prediction models has provided an increased potential for process understanding and model intercomparison on S2S timescales (Vitart et al., 2017; Vitart and Robertson, 2018; Pegion et al., 2019). S2S models tend to be designed based on either weather or climate models and are initialised at a daily to weekly frequency for subseasonal models and a monthly frequency for seasonal models, with lead times generally extending from several weeks for subseasonal models to several months for seasonal models.

On S2S timescales, the potential of stratospheric precursors for tropospheric predictability is however not yet fully exploited, and it also does not always yield improved surface predictions (Domeisen et al., 2020a). This lack of an improvement of the tropospheric predictability after stratospheric events is in part due to a still limited understanding and strong variability of the downward impact (Kolstad et al., 2022) and model biases that make successful predictions on S2S timescales more challenging for both the Northern (Lawrence et al., 2022) and Southern Hemispheres (Bergner et al., 2022). Furthermore, the downward impact and potential for added S2S predictability arising from the stratosphere has been investigated much more extensively for the NH (e.g., Domeisen et al., 2020a) than for the SH. This section explores to what extent predictability on S2S timescales is present in the extratropical SH stratosphere and to what extent this part of the atmosphere can influence predictability at the Earth's surface.

We start with an evaluation of S2S predictability within the stratosphere itself. The stratosphere tends to evolve more slowly as compared to the troposphere, exemplified by the fact that annular mode timescales are longer in the stratosphere than in the troposphere (see Figure 3.2). This slower evolution of the stratosphere is associated with increased predictability of the stratospheric flow as compared to the troposphere (Domeisen et al., 2020b; Son et al., 2020), with the exception of strong disruptions of the stratospheric flow ahead of SSW events, which have shorter deterministic predictable lead times of a few days to roughly two weeks (Domeisen et al., 2020a; Chwat et al., 2022), but which are rare in the SH (Wang et al., 2020; Jucker et al., 2021; Lim et al., 2021). Operational S2S models indicated the 2019 SH SSW event was deterministically predictable two weeks before its onset (Rao et al., 2020c), a longer lead time than the typically observed for NH SSWs.

Figure 3.6 shows a comparison of the prediction timescales for the stratosphere and the troposphere for both hemispheres following the seasonal cycle, mimicking the seasonal cycle of the annular mode timescales in Figure 3.2c,d. The prediction skill is computed from the bias-corrected geopotential height at every level from 30° to 90° latitude of each hemisphere, as an average of all initialisations during a specific month. The skill is defined as the maximum lead time in days when the mean squared error skill score is positive and statistically significant (for details of the computation see Son et al. (2020)). The SH extratropical stratosphere in spring (that is, the period before the final warming) is generally most predictable, followed by the NH stratosphere in mid-winter. On monthly to seasonal timescales, the probability of vortex weakenings in spring can often be successfully estimated and shows skill for forecasts initialised as early as July, as shown for example for the anomalous vortex weakening event in 2019 (Lim et al., 2021). This skill has been traced to the upper stratosphere ahead of the event (Lim et al., 2018).

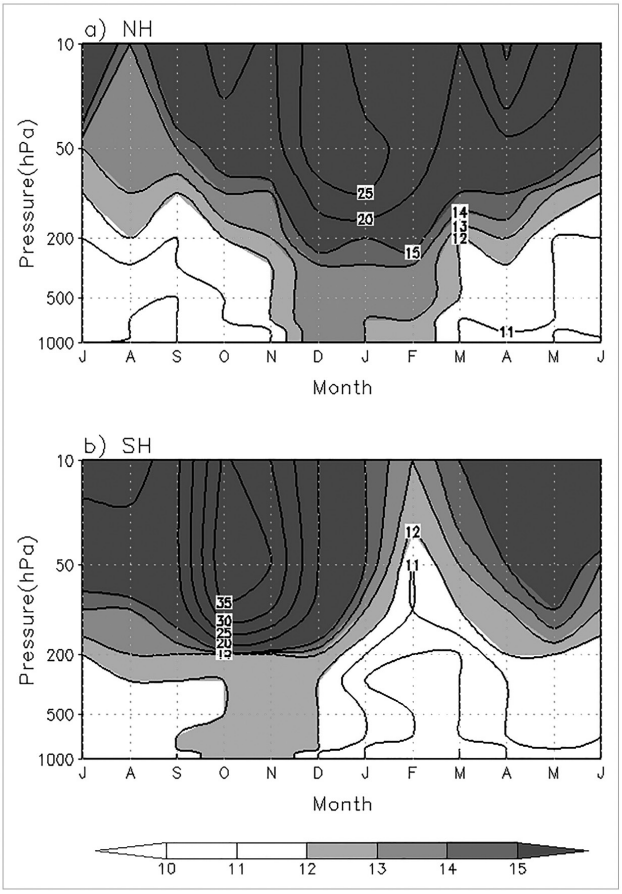

Figure 3.6 Seasonality and vertical structure of prediction skill (in days) for (a) the Northern Hemisphere and (b) the Southern Hemisphere. Contour intervals: 1 day for timescales below 15 days and 5 days for timescales above 15 days. Figure from Son et al. (2020) Note: copyrights not checked for this yet.

The extended stratospheric predictability can benefit tropospheric predictability in case of a downward impact. While a clear downward influence has been shown on longer timescales of interannual and decadal timescales with respect to ozone depletion (Son et al., 2008, 2010; see also Chapter 2), predictability on S2S timescales is also expected, with suggestions that the stratosphere exerts an organising influence onto the troposphere during the final warming event (Black and McDaniel, 2007). Indeed, on seasonal timescales, skillful forecasts of the SH annular mode in the troposphere in spring have been linked to the stratospheric evolution two months prior (Seviour et al., 2014).

Furthermore, the stratosphere can act as a modulator for a range of remote influences that are then communicated to surface climate, including the QBO. Soon after the QBO-MJO connection was rediscovered in 2016, modelling work began to identify a role for the QBO in modulating MJO prediction skill during boreal winter in global subseasonal-to-seasonal

prediction models from Australia (Marshall et al., 2017) and abroad (Lim et al., 2019b; Wang et al., 2019). Across these models, a 5-to-10-day improvement in skill for predicting the bivariate Realtime Multivariate MJO index (Wheeler and Hendon, 2004) was found to occur during QBOE, compared to QBOW (as defined at 50 hPa, also see Section 3.4.2), with a mean model improvement of about one week (Wang et al., 2019). This represents about a 25% improvement in MJO prediction skill when considering the current 4-to-5-week maximum lead time for skilfully predicting the MJO (Kim et al., 2018; Martin et al., 2019). However, there remain challenges to improve such models, making this a topic of ongoing research. Possible reasons for the skill improvement have been proposed, including (1) an increase in the number of strong MJO events during QBOE (which are generally more predictable than weak MJO events), (2) QBOE-QBOW differences in the tropospheric initial conditions, and/or (3) a more persistent MJO during QBOE in the verifying observations (Marshall et al., 2017; Wang et al., 2019; Lim et al., 2019b). Importantly, the model stratosphere may not be a key factor, as the changes in skill are largely unrelated to a model's ability to correctly simulate the QBO (e.g., Wang et al., 2019; Kim et al., 2019). Further, improvements in prediction skill during QBOE versus QBOW may extend outside the tropics by virtue of the MJO's extratropical teleconnections (e.g., Mundhenk et al., 2018; Mayer and Barnes, 2020; Nardi et al., 2020). Thus, understanding the sources of improved MJO skill in QBOE versus QBOW years can ultimately help to improve operational weather and climate predictions globally.

ENSO signals also tend to influence the SH stratospheric circulation (Chapter 11; Simpson et al., 2011b; Domeisen et al., 2019), and can then be communicated back to the surface (Byrne et al., 2019; Stone et al., 2022). These slowly evolving remote influences can further enhance the predictability of the troposphere arising from a stratospheric influence on S2S timescales.

While stratospheric variability has been successfully linked to changes in variability in the troposphere on S2S timescales, especially during SH spring, more research is needed on the predictability of the specific impacts of downward coupling. The most robust signals of downward impact in models are found over Antarctica (Bergner et al., 2022), while Australia also shows impacts of SAM signals arising from stratospheric variability (Lim et al., 2021). Less is known about impacts in other regions, although it is clear that further potential impacts include (but are not limited to) sea ice changes in the Southern Ocean and precipitation anomalies and extremes in South America (Domeisen and Butler, 2020). Given the limited set of mid-winter vortex weakenings in the SH as compared to the NH, robustness is more difficult to establish for the SH response to stratospheric extreme events. However, the high predictability on S2S timescales for spring within the stratosphere and the associated downward impacts promise that a wide range of impacts may still be possible to trace to stratospheric origins, thereby improving predictability for extreme and anomalous surface weather in the extratropical SH.

3.6 Remaining Challenges

The coupling of the stratosphere and the troposphere remains a very active area of research. While we know that the main process for interaction is the propagation and breaking of

atmospheric waves, the fact that the behaviour of those waves both strongly depends on the 'background' state but in turn also directly influences that background state makes it very difficult to obtain a clear idea of causality. In addition, any perturbation within the atmosphere can excite atmospheric waves, making it even more challenging to determine the original source of wave activity. Here, carefully designed modelling experiments can help isolate specific processes, and thereby identify causality. One common theme in all sections from this chapter is that we understand to a good degree how processes related to stratosphere–troposphere coupling work and have made great progress over the last few decades, but many open questions remain, in addition to model deficiencies that should be improved. Some of those are summarised here as a means to close this chapter.

One of the long-standing open questions in stratosphere–troposphere coupling is how exactly the stratospheric signal gets communicated into the troposphere. While we can explain the downward propagation of upper stratospheric anomalies towards the lower stratosphere, it is not clear why the troposphere sometimes does and sometimes does not seem to be influenced by the stratosphere above. And if the troposphere responds to the stratospheric forcing, why is it generally barotropic and why does it not follow the same downward propagation pattern as observed in the stratosphere?

Similarly, but concerning the influence of the QBO on the troposphere, there is a question of how to contextualise results from studies that define QBO regimes based on winds at different pressure levels. To be specific, winds at ∼70 hPa and at ∼20 hPa are often out of phase (Sena et al., 2022); however, QBO composites based on 70 hPa are not equal and opposite to those based on 20 hPa (Gray et al., 2018). Does this lack of equality suggest one level is more important for the underlying mechanism? Or does it imply that the observational record is too short to isolate the true signal from unrelated noise?

The ability of weather forecasting and climate prediction models to capture the QBO-MJO connection relies on their ability to simulate the QBO and MJO individually. Unfortunately, no numerical model to date has been able to reproduce as robustly as observed the characteristics of these climate modes (Kim et al., 2011; Charlton-Perez et al., 2013) or their combined effects (Lim and Son, 2020; Kim et al., 2020a). Model deficiencies such as low spatial resolution, parameterised convection, and missing key physical processes are all possible sources of error (Martin et al., 2021; Lin, 2022). While some global models can qualitatively reproduce the QBO-MJO relationship, their simulated changes in MJO strength due to the QBO are typically less than half of that observed, not statistically significant, or due to noise (Lim et al., 2019b; Kim et al., 2020a). This presents a challenge for exploring the processes that underpin their interactions.

In addition, a point of contention in modelling studies currently exists around whether a simulated QBO-MJO connection reflects the model's ability to capture the underlying physical mechanism behind the relationship (Abhik and Hendon, 2019), or whether it instead arises from the model maintaining a QBO-MJO-influenced observed state in the initial conditions (Wang et al., 2019; Kim et al., 2019). However, some recent work has produced promising results that may help address this question. A cloud-permitting model that represents convective processes with improved realism has demonstrated the ability to better reproduce a QBO-MJO connection than when the model is run at lower

spatial resolution with parameterised convection (Back et al., 2020). Such work points to the likely importance of high resolution with better resolved convection for generating a QBO-MJO link with improved fidelity.

Still staying with the QBO, its extratropical surface impact can be via two distinct pathways, one via the strength of the stratospheric polar vortex, one via tropical convection and related teleconnections. However, the mechanisms underlying both of these pathways are still unclear. Further, while this observed response appears to be robust, it can be masked by sea surface temperature variability, which can overwhelm the QBO-driven signal and make it difficult to isolate a pure QBO signal. Recent work has used modelling studies to dramatically increase the sample size (e.g., Rao et al., 2023). However, Rao et al. (2023) found that not a single model in the CMIP5/6 archive simulated a response to the QBO that is even 60% of that observed. This discrepancy could be due to the difficulty of models to simulate the downward propagation of the QBO to the lowermost stratosphere. Alternately, the observed tropospheric response to the QBO could be, at least in part, influenced by unrelated external forcings or by internal variability. Future work should revisit this question as models improve their representation of the QBO.

Finally, a better representation of the stratospheric circulation in S2S models is expected to benefit the predictability of both the stratosphere and its downward impact onto the troposphere. These improvements include, for example, a reduction in stratospheric biases (Lawrence et al., 2022), higher vertical resolution for an improved representation of gravity waves (Wicker et al., 2023), an increase in the vertical extent of the models (Domeisen et al., 2020b), or interactive ozone (Friedel et al., 2022). But all of these improvements are costly in terms of hardware requirements and compete with the need for finer horizontal resolutions to resolve convective processes.

References

Abhik, S. and Hendon, H. H. (2019). Influence of the QBO on the MJO during coupled model multiweek forecasts. *Geophysical Research Letters*, 46(15), 9213–9221.

Abhik, S., Hendon, H. H. and Wheeler, M. C. (2019). On the sensitivity of convectively coupled equatorial waves to the Quasi-Biennial Oscillation. *Journal of Climate*, 32(18), 5833–5847.

Allen, D. R., Coy, L., Eckermann, S. D., McCormack, J. P., Manney, G. L., Hogan, T. F. and Kim, Y.-J. (2006). NOGAPS-ALPHA simulations of the 2002 Southern Hemisphere stratospheric major warming. *Monthly Weather Review*, 134(2), 498–518.

Andrews, D. G. and McIntyre, M. E. (1976). Planetary waves in horizontal and vertical shear: The generalized eliassen-palm relation and the mean zonal acceleration. *Journal of the Atmospheric Sciences*, 33(11), 2031–2048.

Andrews, D. G. and McIntyre, M. E. (1978). Generalized Eliassen-Palm and Charney-Drazin theorems for waves oin axismmetric mean flows in compressible atmospheres. *Journal of Atmospheric Sciences*, 35(2), 175–185.

Anstey, J. A. and Shepherd, T. G. (2014). High-latitude influence of the Quasi-biennial Oscillation. *Quarterly Journal of the Royal Meteorological Society*, 140(678), 1–21.

Anstey, J. A., Simpson, I. R., Richter, J. H., Naoe, H., Taguchi, M., Serva, F., Gray, L. J., Butchart, N., Hamilton, K., Osprey, S., Bellprat, O., Braesicke, P., Bushell, A. C., Cagnazzo, C., Chen, C., Chun, H., Garcia, R. R., Holt, L., Kawatani, Y., Kerzenmacher,

T., Kim, Y., Lott, F., McLandress, C., Scinocca, J., Stockdale, T. N., Versick, S., Watanabe, S., Yoshida, K. and Yukimoto, S. (2022). Teleconnections of the Quasi-Biennial Oscillation in a multi-model ensemble of QBO-resolving models. *Quarterly Journal of the Royal Meteorological Society*, 148(744), 1568–1592.

Back, S., Han, J. and Son, S. (2020). Modeling evidence of QBO-MJO connection: A case study. *Geophysical Research Letters*, 47(20), e2020GL089480.

Baldwin, M. P. and Dunkerton, T. J. (1998). Quasi-biennial modulation of the southern hemisphere stratospheric polar vortex. *Geophysical Research Letters*, 25(17), 3343–3346.

Baldwin, M. P. and Dunkerton, T. J. (2001). Stratospheric harbingers of anomalous weather regimes. *Science (New York, N.Y.)*, 294(5542), 581–584.

Baldwin, M. P., Gray, L. J., Dunkerton, T. J., Hamilton, K., Haynes, P. H., Randel, W. J., Holton, J. R., Alexander, M. J., Hirota, I., Horinouchi, T., Jones, D. B. A., Kinnersley, J. S., Marquardt, C., Sato, K. and Takahashi, M. (2001). The Quasi-Biennial Oscillation. *Reviews of Geophysics*, 39(2), 179.

Baldwin, M. P., Stephenson, D. B., Thompson, D. W. J., Dunkerton, T. J., Charlton, A. J. and O'Neill, A. (2003). Stratospheric Memory and skill of extended-range weather forecasts. *Science*, 301(5633), 636–640.

Baldwin, M. P. and Thompson, D. W. J. (2009). A critical comparison of stratosphere-troposphere coupling indices. *Quarterly Journal of the Royal Meteorological Society*, 135(644), 1661–1672.

Bandoro, J., Solomon, S., Donohoe, A., Thompson, D. W. J. and Santer, B. D. (2014). Influences of the Antarctic ozone hole on southern hemispheric summer climate change. *Journal of Climate*, 27(16), 6245–6264.

Bergner, N., Friedel, M., Domeisen, D. I. V., Waugh, D. and Chiodo, G. (2022). Exploring the link between austral stratospheric polar vortex anomalies and surface climate in chemistry-climate models. *Atmospheric Chemistry and Physics*, 22(21), 13915–13934.

Black, R. X. and McDaniel, B. A. (2007). Interannual variability in the southern hemisphere circulation organized by stratospheric final warming events. *Journal of the Atmospheric Sciences*, 64(8), 2968–2974.

Breul, P., Ceppi, P. and Shepherd, T. G. (2022). Relationship between southern hemispheric jet variability and forced response: The role of the stratosphere. *Weather and Climate Dynamics*, 3(2), 645–658.

Byrne, N. J. and Shepherd, T. G. (2018). Seasonal persistence of circulation anomalies in the southern hemisphere stratosphere and its implications for the troposphere. *Journal of Climate*, 31(9), 3467–3483.

Byrne, N. J., Shepherd, T. G. and Polichtchouk, I. (2019). Subseasonal-to-seasonal predictability of the southern hemisphere eddy-driven jet during austral spring and early summer. *Journal of Geophysical Research: Atmospheres*, 124(13), 6841–6855.

Byrne, N. J., Shepherd, T. G., Woollings, T. and Plumb, R. A. (2017). Nonstationarity in southern hemisphere climate variability associated with the seasonal breakdown of the stratospheric polar vortex. *Journal of Climate*, 30(18), 7125–7139.

Calvo, N., Polvani, L. M. and Solomon, S. (2015). On the surface impact of arctic stratospheric ozone extremes. *Environmental Research Letters*, 10(9), 094003.

Campitelli, E., Díaz, L. B. and Vera, C. (2022). Assessment of zonally symmetric and asymmetric components of the southern annular mode using a novel approach. *Climate Dynamics*, 58(1–2), 161–178.

Carvalho, L. M. V., Jones, C. and Liebmann, B. (2004). The South Atlantic Convergence Zone: Intensity, form, persistence, and relationships with intraseasonal to interannual activity and extreme rainfall. *Journal of Climate*, 17(1), 88–108.

Ceppi, P. and Hartmann, D. L. (2013). On the speed of the eddy-driven jet and the width of the hadley cell in the southern hemisphere. *Journal of Climate*, 26(10), 3450–3465.
Ceppi, P. and Shepherd, T. G. (2019). The role of the stratospheric polar vortex for the austral jet response to greenhouse gas forcing. *Geophysical Research Letters*, 46(12), 6972–6979.
Charlton-Perez, A. J., Baldwin, M. P., Birner, T., Black, R. X., Butler, A. H., Calvo, N., Davis, N. A., Gerber, E. P., Gillett, N., Hardiman, S., Kim, J., Krüger, K., Lee, Y.-Y. Y., Manzini, E., McDaniel, B. A., Polvani, L. M., Reichler, T., Shaw, T. A., Sigmond, M., Son, S.-W. W., Toohey, M., Wilcox, L., Yoden, S., Christiansen, B., Lott, F., Shindell, D., Yukimoto, S. and Watanabe, S. (2013). On the lack of stratospheric dynamical variability in low-top versions of the CMIP5 models. *Journal of Geophysical Research Atmospheres*, 118(6), 2494–2505.
Charney, J. and Drazin, P. (1961). Propagation of planetary-scale disturbances from the lower into the upper atmosphere. *Journal of Geophysical Research*, 66(1), 83–109.
Christiansen, B., Yang, S. and Madsen, M. S. (2016). Do strong warm ENSO events control the phase of the stratospheric QBO? *Geophysical Research Letters*, 43(19), 489–410.
Chwat, D., Garfinkel, C. I., Chen, W. and Rao, J. (2022). Which sudden stratospheric warming events are most predictable? *Journal of Geophysical Research: Atmospheres*, 127(18), e2022JD037521.
Collimore, C. C., Martin, D. W., Hitchman, M. H., Huesmann, A. and Waliser, D. E. (2003). On the relationship between the QBO and tropical deep convection. *Journal of Climate*, 16(15), 2552–2568.
Domeisen, D. I., Garfinkel, C. I. and Butler, A. H. (2019). The teleconnection of El Niño Southern Oscillation to the stratosphere. *Reviews of Geophysics*, 57(1), 5–47.
Domeisen, D. I. V. and Butler, A. H. (2020). Stratospheric drivers of extreme events at the earth's surface. *Communications Earth & Environment Environment*, 1(59), 1–8.
Domeisen, D. I. V., Butler, A. H., Charlton-Perez, A. J., Ayarzagüena, B., Baldwin, M. P., Dunn-Sigouin, E., Furtado, J. C., Garfinkel, C. I., Hitchcock, P., Karpechko, A. Y., Kim, H., Knight, J., Lang, A. L., Lim, E., Marshall, A., Roff, G., Schwartz, C., Simpson, I. R., Son, S.-W. and Taguchi, M. (2020a). The role of the stratosphere in subseasonal to seasonal prediction: 1. Predictability of the stratosphere. *Journal of Geophysical Research: Atmospheres*, 125(2), e2019JD030920.
Domeisen, D. I. V., Butler, A. H., Charlton-Perez, A. J., Ayarzagüena, B., Baldwin, M. P., Dunn-Sigouin, E., Furtado, J. C., Garfinkel, C. I., Hitchcock, P., Karpechko, A. Y., Kim, H., Knight, J., Lang, A. L., Lim, E.-P., Marshall, A., Roff, G., Schwartz, C., Simpson, I. R., Son, S.-W. and Taguchi, M. (2020b). The role of the stratosphere in subseasonal to seasonal prediction: 2. Predictability arising from stratosphere–troposphere coupling. *Journal of Geophysical Research-Atmospheres*, 125(2), e2019JD030923.
Domeisen, D. I. V., Sun, L. and Chen, G. (2013). The role of synoptic eddies in the tropospheric response to stratospheric variability. *Geophysical Research Letters*, 40(18), 4933–4937.
Dowdy, A. J. (2004). The large-scale dynamics of the mesosphere–lower thermosphere during the southern hemisphere stratospheric warming of 2002. *Geophysical Research Letters*, 31(14), L14102.
Dowdy, A. J., Vincent, R. A., Tsutsumi, M., Igarashi, K., Murayama, Y., Singer, W., Murphy, D. J. and Riggin, D. M. (2007). Polar mesosphere and lower thermosphere dynamics: 2. Response to sudden stratospheric warmings. *Journal of Geophysical Research*, 112(D17), D17105.
Ebdon, R. A. (1960). Notes on the wind flow at 50 mb in tropical and sub-tropical regions in January 1957 and January 1958. *Quarterly Journal of the Royal Meteorological Society*, 86(370), 540–542.

Edmon, H. J., Hoskins, B. J. and McIntyre, M. E. (1980). Eliassen-Palm cross sections for the troposphere. *Journal of the Atmospheric Sciences*, 37(12), 2600–2616.

Eliassen, A. and Palm, T. (1960). On the transfer of energy in stationary mountain waves. *Geofysiske Publikasjoner*, 22(3), 1–23.

Fogt, R. L. and Marshall, G. J. (2020). The Southern Annular Mode: Variability, trends, and climate impacts across the southern hemisphere. *WIREs Climate Change*, 11(4), e652.

Friedel, M., Chiodo, G., Stenke, A., Domeisen, D. I. V., Fueglistaler, S., Anet, J. G. and Peter, T. (2022). Springtime arctic ozone depletion forces northern hemisphere climate anomalies. *Nature Geoscience*, 15(7), 541–547.

Garfinkel, C. I., White, I., Gerber, E. P., Jucker, M. and Erez, M. (2020). The building blocks of northern hemisphere wintertime stationary waves. *Journal of Climate*, 33(13), 5611–5633.

Garfinkel, C. I., White, I., Gerber, E. P., Son, S.-W. and Jucker, M. (2023). Stationary waves weaken and delay the near-surface response to stratospheric ozone depletion. *Journal of Climate*, 36(2), 565–583.

Gerber, E. P., Baldwin, M. P., Akiyoshi, H., Austin, J., Bekki, S., Braesicke, P., Butchart, N., Chipperfield, M., Dameris, M., Dhomse, S., Frith, S. M., Garcia, R. R., Garny, H., Gettelman, A., Hardiman, S. C., Karpechko, A., Marchand, M., Morgenstern, O., Nielsen, J. E., Pawson, S., Peter, T., Plummer, D. A., Pyle, J. A., Rozanov, E., Scinocca, J. F., Shepherd, T. G. and Smale, D. (2010). Stratosphere-troposphere coupling and annular mode variability in chemistry-climate models. *Journal of Geophysical Research*, 115, D00M06.

Gerber, E. P. and Martineau, P. (2018). Quantifying the variability of the annular modes: reanalysis uncertainty vs. sampling uncertainty. *Atmospheric Chemistry and Physics Discussions*, 18(23), 1–28.

Gerber, E. P. and Polvani, L. M. (2009). Stratosphere–troposphere coupling in a relatively simple AGCM: The importance of stratospheric variability. *Journal of Climate*, 22(8), 1920–1933.

Gerber, E. P. and Vallis, G. K. (2007). Eddy–zonal flow interactions and the persistence of the zonal index. *Journal of the Atmospheric Sciences*, 64(9), 3296–3311.

Giorgetta, M. A., Bengtsson, L. and Arpe, K. (1999). An investigation of QBO signals in the east Asian and Indian monsoon in GCM experiments. *Climate Dynamics*, 15(6), 435–450.

Gray, L. J., Anstey, J. A., Kawatani, Y., Lu, H., Osprey, S. and Schenzinger, V. (2018). Surface impacts of the Quasi Biennial Oscillation. *Atmospheric Chemistry and Physics*, 18(11), 8227–8247.

Hartmann, D. L., Holton, J. R. and Fu, Q. (2001). The heat balance of the tropical tropopause, cirrus, and stratospheric dehydration. *Geophysical Research Letters*, 28(10), 1969–1972.

Hartmann, D. L. and Lo, F. (1998). Wave-driven zonal flow vacillation in the southern hemisphere. *Journal of the Atmospheric Sciences*, 55(8), 1303–1315.

Haynes, P., Hitchcock, P., Hitchman, M., Yoden, S., Hendon, H., Kiladis, G., Kodera, K. and Simpson, I. (2021). The influence of the stratosphere on the tropical troposphere. *Journal of the Meteorological Society of Japan*, 99(4), 803–845.

Held, I. M., Ting, M. and Wang, H. (2002). Northern winter stationary waves: Theory and modeling. *Journal of Climate*, 15(16), 2125–2144.

Hendon, H. H. and Abhik, S. (2018). Differences in vertical structure of the Madden-Julian Oscillation associated with the quasi-biennial oscillation. *Geophysical Research Letters*, 45(9), 4419–4428.

Hendon, H. H., Lim, E. and Abhik, S. (2020). Impact of interannual ozone variations on the downward coupling of the 2002 southern hemisphere stratospheric warming. *Journal of Geophysical Research: Atmospheres*, 125(16), e2020JD032952.

Hendon, H. H., Lim, E.-P. and Nguyen, H. (2014). Seasonal variations of subtropical precipitation associated with the southern annular mode. *Journal of Climate*, 27(9), 3446–3460.

Hendon, H. H., Thompson, D. W. J. and Wheeler, M. C. (2007). Australian rainfall and surface temperature variations associated with the southern hemisphere annular mode. *Journal of Climate*, 20(11), 2452–2467.

Hitchcock, P., Shepherd, T. G., Taguchi, M., Yoden, S. and Noguchi, S. (2013). Lower-stratospheric radiative damping and polar-night jet oscillation events. *Journal of the Atmospheric Sciences*, 70(5), 1391–1408.

Hitchman, M. H. and Huesmann, A. S. (2009). Seasonal influence of the quasi-biennial oscillation on stratospheric jets and Rossby wave breaking. *Journal of the Atmospheric Sciences*, 66(4), 935–946.

Holton, J. J. R., Haynes, P. H. P., McIntyre, M. E., Douglass, A. R., Rood, R. B. R., Pfister, L. L. and Douglas, A. (1995). Stratosphere-troposphere exchange. *Reviews of Geophysics*, 33(4), 403–440.

Hong, Y., Liu, G. and Li, J.-L. F. (2016). Assessing the radiative effects of global ice clouds based on CloudSat and CALIPSO measurements. *Journal of Climate*, 29(21), 7651–7674.

Horan, M. F. and Reichler, T. (2017). Modeling seasonal sudden stratospheric warming climatology based on polar vortex statistics. *Journal of Climate*, 30(24), 10101–10116.

Hoskins, B. J. and Ambrizzi, T. (1993). Rossby wave propagation on a realistic longitudinally varying flow. *Journal of the Atmospheric Sciences*, 50(12), 1661–1671.

Hoskins, B. J. and Karoly, D. J. (1981). The steady linear response of a spherical atmosphere to thermal and orographic forcing. *Journal of the Atmospheric Sciences*, 38(6), 1179–1196.

Jucker, M. (2021). Scaling of Eliassen-Palm flux vectors. *Atmospheric Science Letters*, 22(4), e1020.

Jucker, M. and Goyal, R. (2022). Ozone-forced southern annular mode during antarctic stratospheric warming events. *Geophysical Research Letters*, 49(4), e2021GL095270.

Jucker, M. and Reichler, T. (2023). Life cycle of major sudden stratospheric warmings in the southern hemisphere from a multimillennial GCM simulation. *Journal of Climate*, 36(2), 643–661.

Jucker, M., Reichler, T. and Waugh, D. W. (2021). How frequent are antarctic sudden stratospheric warmings in present and future climate? *Geophysical Research Letters*, 48(11), e2021GL093215.

Kalnay, E., Kanamitsu, M., Kistler, R., Collins, W., Deaven, D., Gandin, L., Iredell, M., Saha, S., White, G., Woollen, J., Zhu, Y., Leetmaa, A., Reynolds, R., Chelliah, M., Ebisuzaki, W., Higgins, W., Janowiak, J., Mo, K. C., Ropelewski, C., Wang, J., Jenne, R. and Joseph, D. (1996). The NCEP/NCAR 40-year reanalysis project. *Bulletin of the American Meteorological Society*, 77(3), 437–471.

Kang, S. M., Polvani, L. M., Fyfe, J. C. and Sigmond, M. (2011). Impact of polar ozone depletion on subtropical precipitation. *Science*, 332(6032), 951–954.

Karoly, D. J. and Hoskins, B. J. (1982). Three dimensional propagation of planetary waves. *Journal of the Meteorological Society of Japan. Ser. II*, 60(1), 109–123.

Kim, D., Sobel, A. H., Maloney, E. D., Frierson, D. M. W. and Kang, I.-S. (2011). A systematic relationship between intraseasonal variability and mean state bias in AGCM simulations. *Journal of Climate*, 24(21), 5506–5520.

Kim, H., Caron, J. M., Richter, J. H. and Simpson, I. R. (2020a). The lack of QBO-MJO connection in CMIP6 Models. *Geophysical Research Letters*, 47(11), e2020GL087295.

Kim, H., Richter, J. H. and Martin, Z. (2019). Insignificant QBO-MJO Prediction skill relationship in the SubX and S2S subseasonal reforecasts. *Journal of Geophysical Research: Atmospheres*, 124(23), 12655–12666.

Kim, H., Son, S. and Yoo, C. (2020b). QBO modulation of the MJO-related precipitation in East Asia. *Journal of Geophysical Research: Atmospheres*, 125(4), e2019JD031929.

Kim, H., Vitart, F. and Waliser, D. E. (2018). Prediction of the Madden–Julian Oscillation: A review. *Journal of Climate*, 31(23), 9425–9443.

Klotzbach, P., Abhik, S., Hendon, H. H., Bell, M., Lucas, C., Marshall, A. G. and Oliver, E. C. J. (2019). On the Emerging relationship between the stratospheric quasi-biennial Oscillation and the Madden-Julian oscillation. *Scientific Reports*, 9(1), 2981.

Kolstad, E. W., Lee, S. H., Butler, A. H., Domeisen, D. I. V. and Wulff, C. O. (2022). Diverse surface signatures of stratospheric polar vortex anomalies. *Journal of Geophysical Research: Atmospheres*, 127(20), e2022JD037422.

Kuma, K.-I. (1990). A Quasi-Biennial Oscillation in the intensity of the intra-seasonal oscillation. *International Journal of Climatology*, 10(3), 263–278.

Kushner, P. J. (2010). Annular modes of the troposphere and stratosphere. In: Polvani, L. M., Sobel, A. H. and Waugh, D. W. (eds.) *The Stratosphere: Dynamics, Transport, and Chemistry*, Geophysical Monograph Series, vol. 190, Washington, DC, American Geophysical Union (AGU), pp. 59–91.

Lane, T. P. (2021). Does lower-stratospheric shear influence the mesoscale organization of convection? *Geophysical Research Letters*, 48(3), e2020GL091025.

Lawrence, Z. D., Abalos, M., Ayarzagüena, B., Barriopedro, D., Butler, A. H., Calvo, N., de la Cámara, A., Charlton-Perez, A., Domeisen, D. I. V., Dunn-Sigouin, E. and others (2022). Quantifying stratospheric biases and identifying their potential sources in subseasonal forecast systems. *Weather and Climate Dynamics*, 3(3), 977–1001.

Liess, S. and Geller, M. A. (2012). On the relationship between QBO and distribution of tropical deep convection. *Journal of Geophysical Research: Atmospheres*, 117(D3).

Lim, E.-P., Hendon, H. H., Boschat, G., Hudson, D., Thompson, D. W. J., Dowdy, A. J. and Arblaster, J. M. (2019a). Australian hot and dry extremes induced by weakenings of the stratospheric polar vortex. *Nature Geoscience*, 12(11), 896–901.

Lim, E.-P., Hendon, H. H., Butler, A. H., Thompson, D. W. J., Lawrence, Z. D., Scaife, A. A., Shepherd, T. G., Polichtchouk, I., Nakamura, H., Kobayashi, C., Comer, R., Coy, L., Dowdy, A., Garreaud, R. D., Newman, P. A. and Wang, G. (2021). The 2019 southern hemisphere stratospheric polar vortex weakening and its impacts. *Bulletin of the American Meteorological Society*, 102(6), E1150–E1171.

Lim, E.-P., Hendon, H. H. and Thompson, D. W. (2018). Seasonal evolution of stratosphere-troposphere coupling in the southern hemisphere and implications for the predictability of surface climate. *Journal of Geophysical Research: Atmospheres*, 123(21), 12002–12016.

Lim, Y. and Son, S. (2020). QBO-MJO connection in CMIP5 models. *Journal of Geophysical Research: Atmospheres*, 125(12), e2019JD032157.

Lim, Y., Son, S.-W., Marshall, A. G., Hendon, H. H. and Seo, K.-H. (2019b). Influence of the QBO on MJO prediction skill in the subseasonal-to-seasonal prediction models. *Climate Dynamics*, 53(3–4), 1681–1695.

Lin, H. (2022). The Madden-Julian Oscillation. *Atmosphere-Ocean*, 60(3–4), 338–359.

Liu, Z. and Alexander, M. (2007). Atmospheric bridge, oceanic tunnel, and global climatic teleconnections. *Reviews of Geophysics*, 45(2), RG2005.

Lorenz, D. J. and Hartmann, D. L. (2001). Eddy–zonal flow feedback in the southern hemisphere. *Journal of the Atmospheric Sciences*, 58(21), 3312–3327.

Lubis, S. W., Huang, C. S. Y., Nakamura, N., Omrani, N.-E. and Jucker, M. (2018). Role of finite-amplitude Rossby waves and nonconservative processes in downward migration of extratropical flow anomalies. *Journal of the Atmospheric Sciences*, 75(5), 1385–1401.

Madden, R. A. and Julian, P. R. (1971). Detection of a 40–50 day oscillation in the zonal wind in the tropical Pacific. *Journal of the Atmospheric Sciences*, 28(5), 702–708.

Marshall, A. G., Hendon, H. H., Son, S.-W. and Lim, Y. (2017). Impact of the Quasi-Biennial Oscillation on predictability of the Madden–Julian Oscillation. *Climate Dynamics*, 49(4), 1365–1377.

Martin, Z., Son, S.-W., Butler, A., Hendon, H., Kim, H., Sobel, A., Yoden, S. and Zhang, C. (2021). The influence of the Quasi-Biennial Oscillation on the Madden–Julian Oscillation. *Nature Reviews Earth & Environment*, 2(7), 477–489.

Martin, Z., Wang, S., Nie, J. and Sobel, A. (2019). The impact of the QBO on MJO convection in cloud-resolving simulations. *Journal of the Atmospheric Sciences*, 76(3), 669–688.

Martineau, P. and Son, S.-W. (2015). Onset of circulation anomalies during stratospheric vortex weakening events: The role of planetary-scale waves. *Journal of Climate*, 28(18), 7347–7370.

Matthews, A. J., Hoskins, B. J. and Masutani, M. (2004). The global response to tropical heating in the Madden–Julian Oscillation during the northern winter. *Quarterly Journal of the Royal Meteorological Society*, 130(601), 1991–2011.

Mayer, K. J. and Barnes, E. A. (2020). Subseasonal midlatitude prediction skill following Quasi-Biennial Oscillation and Madden–Julian Oscillation activity. *Weather and Climate Dynamics*, 1(1), 247–259.

McLandress, C., Shepherd, T. G., Scinocca, J. F., Plummer, D. A., Sigmond, M., Jonsson, A. I. and Reader, M. C. (2011). Separating the dynamical effects of climate change and ozone depletion. Part II: Southern hemisphere troposphere. *Journal of Climate*, 24(6), 1850–1868.

Merryfield, W. J., Baehr, J., Batté, L., Becker, E. J., Butler, A. H., Coelho, C. A., Danabasoglu, G., Dirmeyer, P. A., Doblas-Reyes, F. J., Domeisen, D. I., Ferranti, L., Ilynia, T., Kumar, A., Müller, W. A., Rixen, M., Robertson, A. W., Smith, D. M., Takaya, Y., Tuma, M., Vitart, F., White, C. J., Alvarez, M. S., Ardilouze, C., Attard, H., Baggett, C., Balmaseda, M. A., Beraki, A. F., Bhattacharjee, P. S., Bilbao, R., De Andrade, F. M., DeFlorio, M. J., Díaz, L. B., Ehsan, M. A., Fragkoulidis, G., Grainger, S., Green, B. W., Hell, M. C., Infanti, J. M., Isensee, K., Kataoka, T., Kirtman, B. P., Klingaman, N. P., Lee, J. Y., Mayer, K., McKay, R., Mecking, J. V., Miller, D. E., Neddermann, N., Ng, C. H. J., Ossó, A., Pankatz, K., Peatman, S., Pegion, K., Perlwitz, J., Recalde-Coronel, G. C., Reintges, A., Renkl, C., Solaraju-Murali, B., Spring, A., Stan, C., Sun, Y. Q., Tozer, C. R., Vigaud, N., Woolnough, S. and Yeager, S. (2020). Current and emerging developments in subseasonal to decadal prediction. *Bulletin of the American Meteorological Society*, 101(6), E869–E896.

Mindlin, J., Shepherd, T. G., Vera, C. and Osman, M. (2021). Combined effects of global warming and ozone depletion/recovery on southern hemisphere atmospheric circulation and regional precipitation. *Geophysical Research Letters*, 48(12), e2021GL092568.

Mundhenk, B. D., Barnes, E. A., Maloney, E. D. and Baggett, C. F. (2018). Skillful empirical subseasonal prediction of landfalling atmospheric river activity using the Madden–Julian Oscillation and Quasi-Biennial Oscillation. *Npj Climate and Atmospheric Science*, 1(1), 20177.

Naito, Y. (2002). Planetary wave diagnostics on the QBO effects on the deceleration of the polar-night jet in the southern hemisphere. *Journal of the Meteorological Society of Japan. Ser. II*, 80(4B), 985–995.

Nakamura, N. and Zhu, D. (2010). Finite-amplitude wave activity and diffusive flux of potential vorticity in eddy–mean flow interaction. *Journal of the Atmospheric Sciences*, 67(9), 2701–2716.

Nardi, K. M., Baggett, C. F., Barnes, E. A., Maloney, E. D., Harnos, D. S. and Ciasto, L. M. (2020). Skillful all-season S2S prediction of U.S. precipitation using the MJO and QBO. *Weather and Forecasting*, 35(5), 2179–2198.

Nishimoto, E. and Yoden, S. (2017). Influence of the stratospheric Quasi-Biennial Oscillation on the Madden–Julian Oscillation during austral summer. *Journal of the Atmospheric Sciences*, 74(4), 1105–1125.

Oh, J., Son, S.-W., Choi, J., Lim, E.-P., Garfinkel, C., Hendon, H., Kim, Y. and Kang, H.-S. (2022). Impact of stratospheric ozone on the subseasonal prediction in the southern hemisphere spring. *Progress in Earth and Planetary Science*, 9(1), 25.

Pegion, K., Kirtman, B. P., Becker, E., Collins, D. C., LaJoie, E., Burgman, R., Bell, R., DelSole, T., Min, D., Zhu, Y. and others (2019). The subseasonal experiment (SubX): A multimodel subseasonal prediction experiment. *Bulletin of the American Meteorological Society*, 100(10), 2043–2060.

Peña-Ortiz, C., Manzini, E. and Giorgetta, M. A. (2019). Tropical deep convection impact on southern winter stationary waves and its modulation by the Quasi-Biennial Oscillation. *Journal of Climate*, 32(21), 7453–7467.

Plumb, R. A. (1985). On the three-dimensional propagation of stationary waves. *Journal of the Atmospheric Sciences*, 42(3), 217–229.

Polvani, L. M. (2002). Tropospheric response to stratospheric perturbations in a relatively simple general circulation model. *Geophysical Research Letters*, 29(7), 1114.

Polvani, L. M., Waugh, D. W., Correa, G. J. P. and Son, S.-W. (2011). Stratospheric ozone depletion: The main driver of twentieth-century atmospheric circulation changes in the southern hemisphere. *Journal of Climate*, 24(3), 795–812.

Randel, W. J. and Held, I. M. (1991). Phase speed spectra of transient eddy fluxes and critical layer absorption. *Journal of the Atmospheric Sciences*, 48(5), 688–697.

Randel, W. J. and Newman, P. A. (1998). The Stratosphere in the Southern Hemisphere. In: Karoly, D. J. and Vincent, D. G. (eds.), *Meteorology of the Southern Hemisphere*, Meteorological Monographs, Vol. 27. Boston, MA, American Meteorological Society, pp. 243–282.

Rao, J., Garfinkel, C. I., Ren, R., Wu, T. and Lu, Y. (2023). Southern hemisphere response to the quasi-biennial oscillation in the CMIP5/6 models. *Journal of Climate*, 36(8), 2603–2623.

Rao, J., Garfinkel, C. I. and White, I. P. (2020a). How does the quasi-biennial oscillation affect the boreal winter tropospheric circulation in CMIP5/6 models? *Journal of Climate*, 33(20), 8975–8996.

Rao, J., Garfinkel, C. I. and White, I. P. (2020b). Impact of the quasi-biennial oscillation on the northern winter stratospheric polar vortex in CMIP5/6 models. *Journal of Climate*, 33(11), 4787–4813.

Rao, J., Garfinkel, C. I., White, I. P. and Schwartz, C. (2020c). The southern hemisphere minor sudden stratospheric warming in September 2019 and its predictions in S2S models. *Journal of Geophysical Research: Atmospheres*, 125(14), e2020JD032723.

Richter, J. H., Anstey, J. A., Butchart, N., Kawatani, Y., Meehl, G. A., Osprey, S. and Simpson, I. R. (2020). Progress in simulating the quasi-biennial oscillation in CMIP models. *Journal of Geophysical Research: Atmospheres*, 125(8), e2019JD032362.

Roscoe, H. K. and Haigh, J. D. (2007). Influences of ozone depletion, the solar cycle and the QBO on the southern annular mode. *Quarterly Journal of the Royal Meteorological Society*, 133(628), 1855–1864.

Saggioro, E. and Shepherd, T. G. (2019). Quantifying the timescale and strength of southern hemisphere intraseasonal stratosphere-troposphere coupling. *Geophysical Research Letters*, 46(22), 13479–13487.

Sakaeda, N., Dias, J. and Kiladis, G. N. (2020). The unique characteristics and potential mechanisms of the MJO-QBO relationship. *Journal of Geophysical Research: Atmospheres*, 125(17), e2020JD033196.

Scaife, A. A., Baldwin, M. P., Butler, A. H., Charlton-Perez, A. J., Domeisen, D. I. V., Garfinkel, C. I., Hardiman, S. C., Haynes, P., Karpechko, A. Y., Lim, E.-P. and others (2022). Long-range prediction and the stratosphere. *Atmospheric Chemistry and Physics*, 22(4), 2601–2623.

Sena, A. C. T., Peings, Y. and Magnusdottir, G. (2022). Effect of the quasi-biennial oscillation on the Madden Julian Oscillation teleconnections in the southern hemisphere. *Geophysical Research Letters*, 49(6), e2021GL096105.

Seviour, W. J. M., Hardiman, S. C., Gray, L. J., Butchart, N., MacLachlan, C. and Scaife, A. A. (2014). Skillful seasonal prediction of the southern annular mode and antarctic ozone. *Journal of Climate*, 27(19), 7462–7474.

Shaw, T. A., Perlwitz, J. and Harnik, N. (2010). Downward wave coupling between the stratosphere and troposphere: The importance of meridional wave guiding and comparison with zonal-mean coupling. *Journal of Climate*, 23(23), 6365–6381.

Shen, X., Wang, L. and Osprey, S. (2020). Tropospheric forcing of the 2019 Antarctic sudden stratospheric warming. *Geophysical Research Letters*, 47(20), e2020GL089343.

Simpson, I. R., Hitchcock, P., Seager, R., Wu, Y. and Callaghan, P. (2018). The downward influence of uncertainty in the northern hemisphere stratospheric polar vortex response to climate change. *Journal of Climate*, 31(16), 6371–6391.

Simpson, I. R., Hitchcock, P., Shepherd, T. G. and Scinocca, J. F. (2011a). Stratospheric Variability and tropospheric annular-mode timescales. *Geophysical Research Letters*, 38(20).

Simpson, I. R., Shepherd, T. G. and Sigmond, M. (2011b). Dynamics of the lower stratospheric circulation response to ENSO. *Journal of the Atmospheric Sciences*, 68(11), 2537–2556.

Smith, K. L. and Scott, R. K. (2016). The role of planetary waves in the tropospheric jet response to stratospheric cooling. *Geophysical Research Letters*, 43(6), 2904–2911.

Son, S.-W., Gerber, E. P., Perlwitz, J., Polvani, L. M., Gillett, N. P., Seo, K.-H., Eyring, V., Shepherd, T. G., Waugh, D., Akiyoshi, H., Austin, J., Baumgaertner, A., Bekki, S., Braesicke, P., Brühl, C., Butchart, N., Chipperfield, M. P., Cugnet, D., Dameris, M., Dhomse, S., Frith, S., Garny, H., Garcia, R., Hardiman, S. C., Jöckel, P., Lamarque, J. F., Mancini, E., Marchand, M., Michou, M., Nakamura, T., Morgenstern, O., Pitari, G., Plummer, D. A., Pyle, J., Rozanov, E., Scinocca, J. F., Shibata, K., Smale, D., Teyssèdre, H., Tian, W. and Yamashita, Y. (2010). Impact of stratospheric ozone on southern hemisphere circulation change: A multimodel assessment. *Journal of Geophysical Research*, 115, D00M07.

Son, S.-W., Kim, H., Song, K., Kim, S. W., Martineau, P., Hyun, Y. K. and Kim, Y. (2020). Extratropical prediction skill of the subseasonal-to-seasonal (S2S) prediction models. *Journal of Geophysical Research-Atmospheres*, 125(4), e2019JD031273.

Son, S.-W., Lim, Y., Yoo, C., Hendon, H. H. and Kim, J. (2017). Stratospheric control of the Madden–Julian Oscillation. *Journal of Climate*, 30(6), 1909–1922.

Son, S.-W., Polvani, L. M., Waugh, D. W., Akiyoshi, H., GARCIA, R., Kinnison, D., Pawson, S., Rozanov, E., Shepherd, T. G. and Shibata, K. (2008). The impact of stratospheric ozone recovery on the southern hemisphere westerly jet. *Science*, 320(5882), 1486–1489.

Son, S.-W., Purich, A., Hendon, H. H., Kim, B.-M. and Polvani, L. M. (2013). Improved seasonal forecast using ozone hole variability? *Geophysical Research Letters*, 40(23), 6231–6235.

Stolarski, R. S., McPeters, R. D. and Newman, P. A. (2005). The ozone hole of 2002 as measured by TOMS. *Journal of the Atmospheric Sciences*, 62(3), 716–720.

Stone, K. A., Solomon, S., Thompson, D. W., Kinnison, D. E. and Fyfe, J. C. (2022). On the southern hemisphere stratospheric response to ENSO and its impacts on tropospheric circulation. *Journal of Climate*, 35(6), 1963–1981.

Sun, L., Chen, G. and Robinson, W. A. (2014). The role of stratospheric polar vortex breakdown in southern hemisphere climate trends. *Journal of the Atmospheric Sciences*, 71(7), 2335–2353.

Sun, L., Wang, H. and Liu, F. (2019). Combined effect of the QBO and ENSO on the MJO. *Atmospheric and Oceanic Science Letters*, 12(3), 170–176.

Takaya, K. and Nakamura, H. (1997). A formulation of a wave-activity flux for stationary Rossby waves on a zonally varying basic flow. *Geophysical Research Letters*, 24(23), 2985–2988.

Takaya, K. and Nakamura, H. (2001). A formulation of a phase-independent wave-activity flux for stationary and migratory quasigeostrophic eddies on a zonally varying basic flow. *Journal of the Atmospheric Sciences*, 58(6), 608–627.

Thompson, D. W., Baldwin, M. P. and Solomon, S. (2005). Stratosphere–troposphere coupling in the southern hemisphere. *Journal of the Atmospheric Sciences*, 62(3), 708–715.

Thompson, D. W., Solomon, S., Kushner, P. J., England, M. H., Grise, K. M. and Karoly, D. J. (2011). Signatures of the Antarctic ozone hole in southern hemisphere surface climate change. *Nature Geoscience*, 4(11), 741–749.

Thompson, D. W. J. and Wallace, J. M. (2000). Annular modes in the extratropical circulation. Part I: Month-to-month variability. *Journal of Climate*, 13, 1000–1016.

Toms, B. A., Barnes, E. A., Maloney, E. D. and Heever, S. C. (2020). The global teleconnection signature of the Madden-Julian Oscillation and its modulation by the Quasi-Biennial Oscillation. *Journal of Geophysical Research: Atmospheres*, 125(7), e2020JD032653.

Vallis, G. K. (2017). *Atmospheric and Oceanic Fluid Dynamics*. Cambridge: Cambridge University Press.

Vitart, F., Ardilouze, C., Bonet, A., Brookshaw, A., Chen, M., Codorean, C., Déqué, M., Ferranti, L., Fucile, E., Fuentes, M. and others (2017). The Subseasonal to seasonal (S2S) prediction project database. *Bulletin of the American Meteorological Society*, 98(1), 163–173.

Vitart, F. and Robertson, A. W. (2018). The Sub-Seasonal to Seasonal Prediction Project (S2S) and the prediction of extreme events. *Npj Climate and Atmospheric Science*, 1(1), 3.

Wang, J., Kim, H., Chang, E. K. M. and Son, S. (2018). Modulation of the MJO and North Pacific storm track relationship by the QBO. *Journal of Geophysical Research: Atmospheres*, 123(8), 3976–3992.

Wang, L., Hardiman, S. C., Bett, P. E., Comer, R. E., Kent, C. and Scaife, A. A. (2020). What chance of a sudden stratospheric warming in the southern hemisphere? *Environmental Research Letters*, 15(10), 104038.

Wang, S., Tippett, M. K., Sobel, A. H., Martin, Z. K. and Vitart, F. (2019). Impact of the QBO on prediction and predictability of the MJO convection. *Journal of Geophysical Research: Atmospheres*, 124(22), 11766–11782.

Wheeler, M. C. and Hendon, H. H. (2004). An All-Season Real-Time Multivariate MJO Index: Development of an index for monitoring and prediction. *Monthly Weather Review*, 132(8), 1917–1932.

White, R., Wallace, J. and Battisti, D. (2021). Revisiting the role of mountains in the northern hemisphere winter atmospheric circulation. *Journal of the Atmospheric Sciences*, 78(7), 2221–2235.

Wicker, W., Polichtchouk, I. and Domeisen, D. I. V. (2023). Increased vertical resolution in the stratosphere reveals role of gravity waves after sudden stratospheric warmings. *Weather and Climate Dynamics*, 4(1), 81–93.

Yamashita, Y., Naoe, H., Inoue, M. and Takahashi, M. (2018). Response of the southern hemisphere atmosphere to the stratospheric equatorial Quasi-Biennial Oscillation (QBO) from winter to early summer. *Journal of the Meteorological Society of Japan. Ser. II*, 96(6), 587–600.

Yamazaki, K. and Nakamura, T. (2021). The stratospheric QBO affects antarctic sea ice through the tropical convection in early austral winter. *Polar Science*, 28, 100674.

Yang, H., Sun, L. and Chen, G. (2015). Separating the mechanisms of transient responses to stratospheric ozone depletion–like cooling in an idealized atmospheric model. *Journal of the Atmospheric Sciences*, 72(2), 763–773.

Yang, Q., Fu, Q. and Hu, Y. (2010). Radiative impacts of clouds in the tropical tropopause layer. *Journal of Geophysical Research*, 115, D00H12.

Yoo, C. and Son, S. (2016). Modulation of the boreal wintertime Madden-Julian Oscillation by the stratospheric Quasi-Biennial Oscillation. *Geophysical Research Letters*, 43(3), 1392–1398.

Zhang, C. and Zhang, B. (2018). QBO-MJO connection. *Journal of Geophysical Research: Atmospheres*, 123(6), 2957–2967.